

Award Number: W81XWH-06-1-0314

TITLE: Breast Cancer Lymphatic Dissemination-Influence of Estrogen and Progesterone

PRINCIPAL INVESTIGATOR: Joshua C. Harrell
Kathryn B. Horwitz, Ph.D.

CONTRACTING ORGANIZATION: University of Colorado Health Sciences Center
Aurora, CO 80045-0508

REPORT DATE: March 2007

TYPE OF REPORT: Annual Summary

PREPARED FOR: U.S. Army Medical Research and Materiel Command
Fort Detrick, Maryland 21702-5012

DISTRIBUTION STATEMENT: Approved for Public Release;
Distribution Unlimited

The views, opinions and/or findings contained in this report are those of the author(s) and should not be construed as an official Department of the Army position, policy or decision unless so designated by other documentation.

REPORT DOCUMENTATION PAGE

Form Approved
OMB No. 0704-0188

Public reporting burden for this collection of information is estimated to average 1 hour per response, including the time for reviewing instructions, searching existing data sources, gathering and maintaining the data needed, and completing and reviewing this collection of information. Send comments regarding this burden estimate or any other aspect of this collection of information, including suggestions for reducing this burden to Department of Defense, Washington Headquarters Services, Directorate for Information Operations and Reports (0704-0188), 1215 Jefferson Davis Highway, Suite 1204, Arlington, VA 22202-4302. Respondents should be aware that notwithstanding any other provision of law, no person shall be subject to any penalty for failing to comply with a collection of information if it does not display a currently valid OMB control number. **PLEASE DO NOT RETURN YOUR FORM TO THE ABOVE ADDRESS.**

1. REPORT DATE 01-03-2007			2. REPORT TYPE Annual Summary		3. DATES COVERED 1 Mar 2006 – 28 Feb 2007	
4. TITLE AND SUBTITLE Breast Cancer Lymphatic Dissemination-Influence of Estrogen and Progesterone					5a. CONTRACT NUMBER	
					5b. GRANT NUMBER W81XWH-06-1-0314	
					5c. PROGRAM ELEMENT NUMBER	
6. AUTHOR(S) Joshua C. Harrell Kathryn B. Horwitz, Ph.D. Email: Joshua.Harrell@uchsc.edu					5d. PROJECT NUMBER	
					5e. TASK NUMBER	
					5f. WORK UNIT NUMBER	
7. PERFORMING ORGANIZATION NAME(S) AND ADDRESS(ES) University of Colorado Health Sciences Center Aurora, CO 80045-0508					8. PERFORMING ORGANIZATION REPORT NUMBER	
					10. SPONSOR/MONITOR'S ACRONYM(S)	
					11. SPONSOR/MONITOR'S REPORT NUMBER(S)	
12. DISTRIBUTION / AVAILABILITY STATEMENT Approved for Public Release; Distribution Unlimited						
13. SUPPLEMENTARY NOTES Original contains colored plates: ALL DTIC reproductions will be in black and white.						
14. ABSTRACT Breast cancers commonly spread to lymph nodes (LNs). If the primary tumors are estrogen receptor (ER) and/or progesterone receptor (PR) positive, then the likelihood that LN metastases express receptors exceeds 80%. However, due to lack of ER+ models, little is known about the role of hormones in breast cancer spread or the effects of the LN microenvironment on hormone responsiveness. We have developed metastasis models using ZsGreen labeled MCF-7 and T47D human breast cancer cells. Tumors are tracked in living mice by whole-body imaging, and macrometastases or micrometastases are detected by intravital imaging or fluorescence microscopy. Tumor growth is estrogen dependent and required for intratumoral lymphangiogenesis. Seventy-five percent of all tumors and >95% of larger tumors generate LN metastases. Occasionally more distant metastases are also observed. "Triads" of primary tumors, tumor-filled draining lymphatic vessels, and tumor-filled LNs from the same mouse show that (a) proliferation, as measured by 5-bromo-2'-deoxyuridine uptake, is higher in the LN than in the primary tumor. (b) High ER levels are extensively down-regulated by estradiol in primary tumors. However, there is partial failure of ER down-regulation in LNs associated with (c) reduced PR expression. This suggests that ER are dysfunctional in the LN microenvironment and perhaps hormone resistant. (d) CD44 is sparsely expressed in primary tumor cells but homogeneously overexpressed in cells transiting the lymphatics and populating LNs. We hypothesize that CD44 expression targets tumor cells for transport to, and uptake in, LNs. If so, the CD44 pathway could be targeted therapeutically to slow or prevent LN metastases.						
15. SUBJECT TERMS ER, PR, lymph node, metastasis, fluorescent proteins						
16. SECURITY CLASSIFICATION OF:				17. LIMITATION OF ABSTRACT	18. NUMBER OF PAGES	19a. NAME OF RESPONSIBLE PERSON
a. REPORT	b. ABSTRACT	c. THIS PAGE	USAMRMC			
U	U	U	UU	35	19b. TELEPHONE NUMBER (include area code)	

Table of Contents

Introduction.....	4
Body.....	5
Key Research Accomplishments.....	9
Reportable Outcomes.....	10
Conclusion.....	10
References.....	10
Appendices.....	11

Introduction

Breast cancer spread into the lymph nodes (LN) is the single most deadly prognostic factor identified to date. Understanding factors that regulate cancer-cell colonization of the lymphatics is essential to prevent malignant invasion. Most breast cancers are estrogen (ER) and/or progesterone receptor (PR) positive, and the majority of breast cancers that spread to the LN maintain ER and PR. However, due to lack of experimental models of ER+ breast cancer metastasis, little is known about the roles of hormones in breast cancer spread to, and growth in, LNs.

Hypotheses: I postulate that breast cancer metastasis to LN is dependent on tumor growth and tumor size. Second, I predict that tumor spread to LNs is dependent on tumor associated lymphangiogenesis. Finally, I hypothesize that ER expression and transcriptional function is maintained in tumors and LN metastases.

Project goals: I plan to develop and then define models of ER+ breast cancer metastasis, in preparation for studies of hormone action that will address hormonal regulation of key genes involved in lymphatic development, LN spread, and growth of cancer cells within the LNs.

Approved STATEMENT OF WORK:

Task 1. Develop and characterize all cell lines used in the study (Months 1-6).

- A. Make ZsGreen and DsRed-Express polyclonal stable cell lines.**
- B. Quantitation of ER and PR protein expression in each lines.**

Task 2. Assess the impact of systemic estrogen and progesterone on ER+/- PR+/- breast cancer lymphatic spread (Months 6-36).

- A. Grow and determine the rate of lymphatic invasion using homogeneous or dual colored mixed ER+/-, PR+/- tumors with no systemic hormones, E, P, E+P.**
- B. Perform immunohistochemistry on tumors, lymphatics, and LNs to understand effects of E and P on cancer cells, lymphatics, and LNs.**

Task 3. Determine hormonal influence to tumor lymphangiogenesis (Months 8-36).

- A. Determine hormone influence on gene expression of lymphangiogenic factors.**
- B. Immunohistochemically quantitate lymph vessels in each tumor line and determine the influence of hormones on lymphatic vessel development.**

Body

Task 1. The majority of the work to date is summarized in my first author publication enclosed within the appendix, “Estrogen receptor positive breast cancer metastasis: Altered hormonal sensitivity and tumor aggressiveness in lymphatic vessels and lymph nodes” (1). In this paper I describe the studies that complete task 1 of the approved statement of work. This includes; (a) fluorescently labeling ER+ breast cancer cells (MCF-7 and T47D) with ZsGreen and DsRed-Express, and, (b) immunohistochemically quantifying the amounts of ER and PR expression in the breast cancer cells grown *in vivo*.

The methods used to complete the statement of work for task 1A, the labeling of the cancer cells with green and red fluorescent proteins, was done through generating packaging cells that produced ZsGreen or DsRedExpress retrovirus. To obtain potent retrovirus, I found it necessary to use fluorescence associated cell sorting (FACS) to isolate out the brightest packaging cells that subsequently produce the most virus. I used this approach for both the red and green packaging cells. Overlaying the virus on the cancer cells required multiple rounds of transduction for them to turn green or red. After transduction the cells were selected and a homogenously fluorescent polyclonal population was isolated by FACS. These cells were then expanded and frozen down into multiple bullets so that every *in vivo* experiment would be conducted from the same passage number cell lines.

The methods used to complete the statement of work for task 1B, which included the immunohistochemical quantification of the levels of MCF-7 ER and PR in the MCF7 cancer cells, were reported in detail in my first author publication (1). In short, ER were highly expressed in mammary gland tumors of all estradiol-free mice. However, ligand-dependent downregulation of ER was observed in tumors upon estradiol supplementation. This downregulation corresponded with PR expression, demonstrating the correlation between ligand dependent downregulation of ER and its transcriptional activity. Surprisingly, these expression patterns were altered in metastases within the lymphatic vessels or in LNs, with increased ER and decreased PR in lymphatic metastases. This suggests that the lymphatic environment makes ER+ cancer cells estrogen insensitive (Harrell et al, figure 6). These finding led me to conduct follow-up studies that are currently underway. In addition, it should be mentioned that the route of metastatic dissemination was identical between the MCF-7 and T47D cell lines. These studies complete task 1.

Task 2. The second task in my approved statement of work is to assess the impact of systemic estrogen and progesterone on ER+/- PR+/- breast cancer lymphatic spread (Months 6-36). Results concluded so far are documented in detail in my first author paper (1). In short, so far I have investigated the requirement of estradiol in stimulating tumor growth and LN metastases. Using both ER+ MCF-7 and T47D human breast cancer cells we found that estradiol

was strictly required for tumor growth and subsequent LN metastasis (Harrell et al, figure 3). Immunohistochemistry (task 2b), found differences in ER and PR expression in tumors and lymphatic metastases (previously discussed).

Now that I have characterized the effects of estradiol alone on tumor growth and LN spread, over the next 12 months I will initiate studies that investigate how progesterone alone or in combination affect ER+ tumor growth and metastasis. The findings of reduced PR expression (from task 1 above) in metastases suggests that treating mice with estradiol + progesterone may not affect cancer cells any differently once they become metastatic—as the amount of PR that can bind progesterone is diminished. Nevertheless, since primary MCF-7 tumors express PR upon estradiol treatment it will be interesting to know if tumor growth or cancer cell entry into lymphatics is altered by the addition of progesterone with estradiol, or with progesterone alone.

Once the studies investigating the roles of progesterone +/- estradiol in LN metastasis are underway and providing information, I will then expand the model and incorporate the use of ER- cell lines individually and in combination with ER+ cell lines. The goal of these studies will be to determine if tumors containing mixed ER+ and ER- cells behave differently from pure tumor cell populations and inform us if ER and PR potentially regulate different paracrine factors that impact tumor growth and spread.

Task 3. The third task in my approved statement of work is to determine hormonal influence on tumor lymphangiogenesis. In my first-author publication I show that estradiol dependent tumor growth correlates with intratumoral lymphangiogenesis (Harrell et al, Figure 4), where intratumoral lymphatic vessels were only identified in estradiol treated MCF-7 tumors. Peritumoral LVs were found surrounding nearly all tumors, regardless of hormone treatment, and likely derived from the normal lymphatic vasculature that makes up the mammary gland. Interestingly, not all tumors that contained peri- or intratumoral lymphatic vessels generated LN metastasis, and tumors that were found to not contain intratumoral lymphatic vessels also shed metastases. From these results we conclude that estradiol-dependent tumor growth correlates with intratumoral lymphatic vessel development, however, presence of these vessels is not required for LN colonization. Over the next 12 months I plan to determine the influence of hormones on gene expression of known lymphangiogenic factors. Through global gene expression profiling and/or RT-PCR I will determine if any of the known lymphangiogenic factors that are secreted by cancer cells are influenced by estradiol or progesterone.

Ongoing studies. Based on the findings of apparent estradiol insensitivity observed in ER+ LN metastasis described in Harrell et al., (1), I have initiated studies to further investigate if estradiol signaling through ER is different between cancer cells that comprise mammary glands versus cancer cells that have metastasized to the LN. Through an expansion of the current *in vivo* tumor

growth and metastasis model, I have designed experiments that will identify the genes that are estradiol regulated in MCF-7 tumors and their matched LN metastases. Data from these studies will help fulfill requirements for tasks 2 &3 and will help determine the mechanisms that contribute to heightened proliferation rates and CD44 expression observed in LN metastases (Harrell et al.). In this model the tumors will be grown with estradiol supplementation until they generate axillary LN metastasis, upon which time half of the mice will undergo a one- or four-week estradiol withdrawal procedure. Estrogenized mice, and those that have undergone estradiol withdrawal, will have their tumors and LNs containing metastases removed, subjected to laser-capture microdissection, and analyzed by microarray analysis. The laser-capture microarray procedure will be required to isolate and further analyze equal numbers of human cancer cells growing as tumors and LN metastases. These studies are currently underway. An example of how these cells will be identified and captured is shown in figure 1.

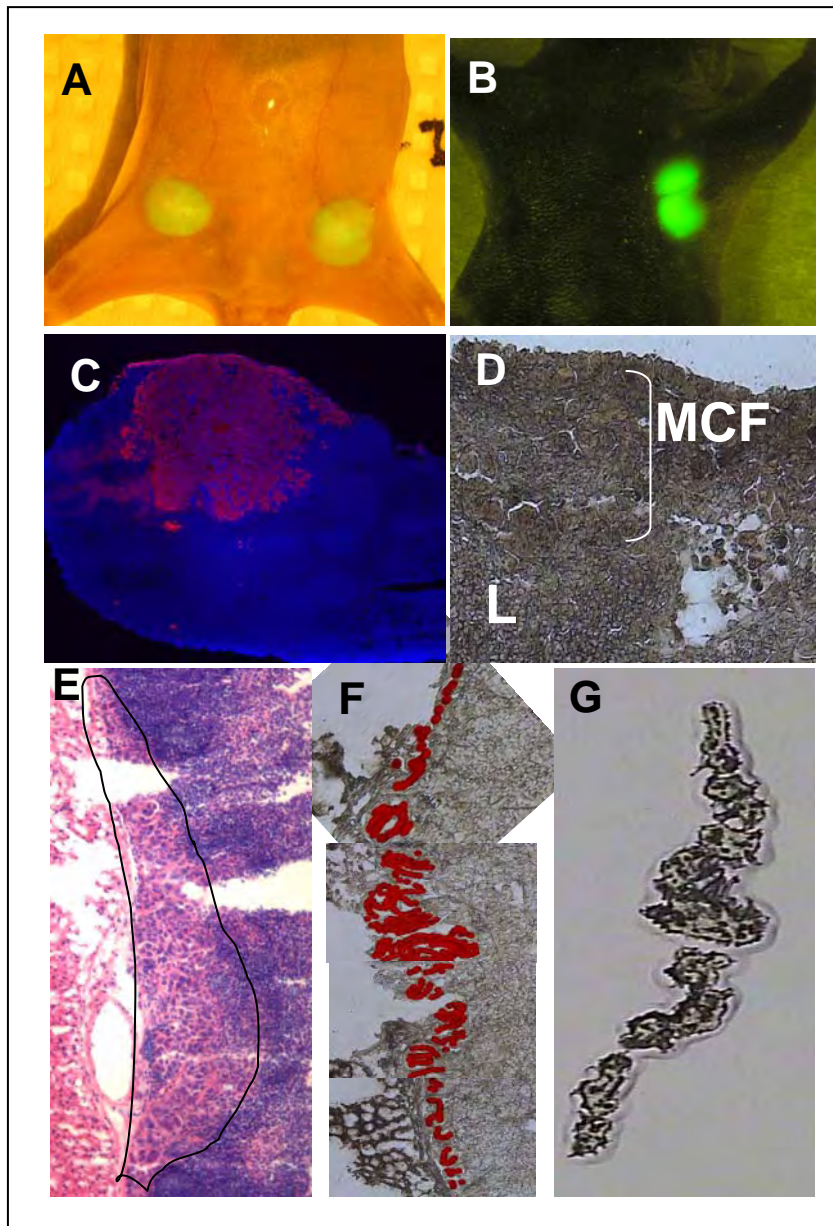


Figure 1. Identification of MCF7+ZsGreen cells in tumors and LN metastases for laser capture isolation. *A*, Fluorescent whole body image of bilateral MCF7+ZsGreen tumors. *B*, Fluorescent whole body image of MCF7+ZsGreen metastasis to the left axillary LN. *C*, Fluorescence IHC for cytokeratin 18 (red) and DAPI (blue) of an axillary LN metastasis (4x). *D*, White-light laser capture microscope image of an axillary LN metastasis showing MCF-7 cells or lymphocytes (Ly) (40x). *E*, H&E of a MCF-7 LN metastasis. *F*, Serial section with MCF-7 cells marked for laser capture. *G*, Captured cancer cells.

Key Research Accomplishments

- Publications: One first author, two second author.

Harrell JC, Dye WW, Allred DC, Jedlicka P, Spoelstra NS, Sartorius CA, Horwitz KB. Estrogen receptor positive breast cancer metastasis: altered hormonal sensitivity and tumor aggressiveness in lymphatic vessels and lymph nodes. *Cancer Res.* 2006 Sep 15;66(18):9308-15.

Jacobsen BM, **Harrell JC**, Jedlicka P, Borges VF, Varella-Garcia M, Horwitz KB. Spontaneous fusion with, and transformation of mouse stroma by, malignant human breast cancer epithelium. *Cancer Res.* 2006 Aug 15;66(16):8274-9.

Massart F, **Harrell JC**, Federico G, Saggese G. Thyroid outcome during long-term gonadotropin-releasing hormone agonist treatments for idiopathic precocious puberty. *J Adolesc Health.* 2007 Mar;40(3):252-7. Epub 2007 Jan 5.

- Meetings attended

2006 Gordon Conference: Molecular Mechanisms in Lymphatic Function & Disease. September 3, 2006-September 8, 2006. Les Diablerets, Switzerland.

2007 Keystone Symposia: Host cell Interaction and Response to the Cancer Cell. January 21-26, 2007. Keystone, Colorado.

- Awards

2007 United States National Science Foundation & Australian Academy of Sciences East Asian and Pacific Summer Institutes. June 13-August 8 2007, University of Adelaide, Adelaide, Australia.

1st place student poster: 2006 University of Colorado Health Sciences Center's Department of Medicine Fourth Annual Research Day. October 21, 2006, Aurora, Colorado.

2nd place poster: 2006 University of Colorado Health Sciences Center's Department of Cellular and Developmental Biology Annual Retreat. September 2006, Estes Park, Colorado.

2006 UCHSC C. Werner and Kitty Hirs Research Award for PhD Student Travel to National Meetings.

Reportable Outcomes

1-First Author Manuscripts

Harrell JC, Dye WW, Allred DC, Jedlicka P, Spoelstra NS, Sartorius CA, Horwitz KB. Estrogen receptor positive breast cancer metastasis: altered hormonal sensitivity and tumor aggressiveness in lymphatic vessels and lymph nodes. *Cancer Research*. 2006 Sep 15;66 (18):9308-15.

2-Abstracts

2006 Gordon Conference: Molecular mechanisms in lymphatic function and disease. Les Diablerets, Switzerland.

2007 Keystone Symposia: Host cell interaction and response to the cancer cell. Keystone, Colorado.

3-Funding applied for based on the work supported by this training grant

2007 DOD Breast Cancer Research Program Concept Award

Applied: February 6, 2007. This grant aims to expand on the development of the fluorescent breast cancer lymphatic metastasis models by generating more distant models of breast cancer metastasis. If funded these studies will parallel the lymphatic metastasis studies currently ongoing, but will be distinct in that they will focus on distant blood vessel derived metastases.

Conclusions

The first year of the funding (March 1 2006-March 1, 2007) for the predoctoral grant BC050889 was highly successful. The research conducted yielded exciting results and the development of the first known reliable model of ER+ breast cancer metastasis *in vivo*. This model and methods have since led to the establishment of collaborations with numerous investigators at UCHSC. Initial results found that there are differences in estrogen responsiveness in breast tumors compared to the matched LN metastases, suggesting that aromatase inhibitors and other estrogen/ER mediated therapies may be differentially affecting cancer cells—dependent on their tissue location.

Reference

Joshua Chuck Harrell, Wendy W. Dye, D. Craig Allred, Paul Jedlicka, Nicole S. Spoelstra, Carol A. Sartorius, and Kathryn B. Horwitz. *Estrogen Receptor Positive Breast Cancer Metastasis: Altered Hormonal Sensitivity and Tumor Aggressiveness in Lymphatic Vessels and Lymph Nodes*. *Cancer Research*, 2006; 66: (18). September 15, 2006.

Appendices

1. NIH Biosketch.
2. Abstracts for meetings attended.
3. Three publications from the past 12 months.

BIOGRAPHICAL SKETCH

NAME J Chuck Harrell	POSITION TITLE Graduate Student-Doctoral Candidate		
eRA COMMONS USER NAME			
EDUCATION/TRAINING <i>(Begin with baccalaureate or other initial professional education, such as nursing, and include postdoctoral training.)</i>			
INSTITUTION AND LOCATION	DEGREE <i>(if applicable)</i>	YEAR(s)	FIELD OF STUDY
North Carolina State University-Raleigh, NC, US	BS	2000	Biological Sciences
University of Colorado Health Sciences Center- Aurora, CO, US	PhD	2007	Reproductive Sciences

RESEARCH AND PROFESSIONAL EXPERIENCE

National Institutes of Environmental Health Sciences, Research Triangle Park, NC, USA
Undergraduate Internship (September 1998-June 1999, August 1999-December 2000)
Intramural Recreational Training Award (December 2000-July 2002)

North Carolina Division of Marine Fisheries, Morehead City, NC, USA
NC State Government Summer Internship Program (June 1999-August 1999)

University of Colorado Health Sciences Center, Aurora, CO, USA
Graduate Student (2002-Present)
Doctoral Candidate (2005-Present)

AWARDS

U.S. Department of Defense Breast Cancer Training Grant (September 2003-August 2004)

Avon Scholar (2005-Present)

U.S. Department of Defense Breast Cancer Predoctoral Training Awardee (March 2006-March 2009)

1st place poster: 2005 Cell and Developmental Biology and Program in Reproductive Sciences Annual Retreat

C. Werner and Kitty Hirs 2006 Research Award for PhD Student Travel to National Meetings

2nd place poster: 2006 Cell and Developmental Biology and Program in Reproductive Sciences Annual Retreat

1st place poster: 2006 UCHSC Department of Medicine Research Day

*U. S. National Science Foundation East Asia and Pacific Summer Institute in Australia
(6/2007-8/2007)*

RESEARCH CONFERENCES ATTENDED

2003 Keystone Symposia-Nuclear Receptors: Steroid Hormones, Keystone, CO, US
2005 Speaker-25th Annual San Antonio Breast Cancer Symposia, San Antonio, TX, US
2006 Poster Presenter-Gordon Conference: Molecular mechanisms in lymphatic function and disease, Les Diablerets, Switzerland
2007 Poster Presenter-Keystone Symposia: Host cell interaction and response to the cancer cell, Keystone, CO, US

PUBLICATIONS

Harrell JC, Sartorius CA, Dye WW, Jacobsen BM, Horwitz KB. ZsGreen labeling of breast cancer cells to visualize metastasis. In Press, Clontechniques. April 2007.

Massart F, Federico G, Harrell JC, Saggese G. Thyroid outcome during long-term gonadotropin-releasing hormone agonist treatments for idiopathic precocious puberty. In press, Journal of Adolescent health. 2007.

Harrell JC, Dye WW, Allred DC, Jedlicka P, Spoelstra NS, Sartorius CA, Horwitz KB. Estrogen receptor positive breast cancer metastasis: altered hormonal sensitivity and tumor aggressiveness in lymphatic vessels and lymph nodes. Cancer Research. 2006 Sep 15;66 (18):9308-15.

Jacobsen BM, Harrell JC, Jedlicka P, Borges VF, Varella-Garcia M, Horwitz KB. Spontaneous fusion with, and transformation of mouse stroma by, malignant human breast cancer epithelium. Cancer Research. 2006 Aug 15;66 (16):8274-9.

Hewitt SC, Harrell JC, Korach KS. Lessons in estrogen receptor biology from knockout and transgenic animals. Annual Review of Physiology. Volume 67, 2005: 285-308.

Massart F, Harrell JC, Federico G, Saggese G. Human breast milk and xenoestrogen exposure: a possible impact on human health. J Perinatol. 2005 Apr; 25(4):282-8.

Melvin VS, Harrell C, Adelman JS, Kraud WL, Churchill M, Edwards DP. The role of the C-terminal extension (CTE) of the estrogen receptor alpha and beta DNA binding domain in DNA binding and interaction with HMGB. J Biol Chem. 2004 Apr 9;279(15):14763-71.

Korach KS, Emmen JM, Walker VR, Hewitt SC, Yates M, Hall JM, Swope DL, Harrell JC, Couse JF. Update on animal models developed for analyses of estrogen receptor biological activity. J Steroid Biochem Mol Biol. 2003 Sep;86(3-5):387-91.

Swope D, Harrell JC, Mahato D, Korach KS. Genomic structure and identification of a truncated variant message of the mouse estrogen receptor alpha gene. Gene. 2002 Jul 10;294(1-2)239-47.

Hewitt SC, Bocchinfuso WP, Shai J, Harrell C, Koonce L, Clark J, Myers P, Korach KS. Lack of ductal development in the absence of functional estrogen receptor alpha delays mammary tumor formation induced by transgenic expression of ErbB2/neu. Cancer Research. 2002 May 15;62(10):2798-805.

Swope DL, Castranio T, Harrell JC, Mishina Y, Korach KS. AF-2 knock-in mutation of estrogen receptor alpha: Cre-loxP excision of a PGK-neo cassette from the 3'UTR. *Genesis*. 2002 Feb;32(2):99-101.

Abstracts of Meetings Attended

2006 Gordon Conference: Molecular mechanisms in lymphatic function and disease

J. Chuck Harrell, Wendy W. Dye, Carol A. Sartorius, Kathryn B. Horwitz.
Department of Medicine and Program in Reproductive Sciences, University of Colorado Health Sciences Center, Aurora, CO, USA 80010

Characterizing a model of estrogen-dependent breast cancer lymphatic metastasis

Background: Breast cancer metastasis kills over 400,000 women worldwide each year. The first location breast cancers spread to are usually the lymph nodes. Seventy-five percent of primary breast tumors are estrogen (ER) and/or progesterone receptor (PR) positive and nearly all lymph node metastases retain ER/PR. To date, no models have been employed to study the effects of hormones on cancer cell movement through lymphatic vessels into lymph nodes.

Methods: ER+/PR+ human breast cancer cells (MCF-7, T47D) were retrovirally labeled to express the new fluorescent proteins ZsGreen or DsRed-Express. To establish tumors, the abdominal mammary glands of ovariectomized nude mice were injected with one-million fluorescent cancer cells in 100% matrigel. Mice were untreated or supplemented with estradiol for up to 12 weeks. Tumor growth and lymphatic dissemination were monitored weekly with fluorescent whole body imaging, and intravital fluorescence microscopy identified metastases at necropsy. These techniques allowed us to isolate matched trios of tumors, lymphatic vessel emboli, and lymph node metastases.

Results: Tumor growth and lymph node spread of both cell lines was estrogen dependent. Seventy percent of estrogen treated tumors yielded metastases that could be monitored in living mice without the use of anesthetics. In the primary tumors, estrogen-induced tumor growth was found to induce intratumoral lymphangiogenesis. ER expression was drastically reduced with estrogen supplementation and this coincided with heterogeneous expression of PR. In estrogenized states the lymphatic emboli expressed tumor-like proportions of ER and PR, whereas the lymph node metastases had slightly increased ER levels and reduced PR expression. BrdU labeling showed proliferation rates that were equivalent in tumors and lymphatic emboli; lymph node metastases however, exhibited a 42% increase in proliferation rate compared to the primary tumor from the same mouse.

Discussion: We have developed a model of ER+/PR+ breast cancer lymph node metastasis that allows for study of hormone regulation of this process within the tumor, the lymphatics and lymph nodes. Equivalent ER, PR, and proliferation rates in the primary tumor and lymphatic vessel emboli suggests that ER+ breast cancers need not lose estrogen responsiveness for lymphatic metastasis. These data also suggest that the lymph node microenvironment may contribute to the physiology of metastatic cancers. DOD grant to JCH BC050889.

2007 Keystone Symposia: Host cell interaction and response to the cancer cell

Estrogen regulates different sets of genes in primary breast tumors and their lymph node metastases

J. Chuck Harrell, Wendy W. Dye, Djuana M. E. Harvell, Carol A. Sartorius, Kathryn B. Horwitz. Department of Medicine and Program in Reproductive Sciences, University of Colorado Health Sciences Center, Aurora, CO, USA 80010

The majority of primary breast tumors and their metastases are estrogen receptor positive. Spread to lymph nodes (LN) indicates advanced disease, often foreshadowing further spread. To understand how hormones impact this process we established a fluorescent xenograft model of estrogen-dependent human breast cancer metastasis. Initial studies indicated increased proliferation rate and decreased estrogen-dependent progesterone receptor expression in lymphatic vessel (LV) and LN metastases compared to their matched primary tumors, suggesting that each microenvironment uniquely influences cancer aggressiveness. To determine genomic targets that control enhanced aggressiveness in LNs, matched pairs of primary tumors and their LN metastases from estradiol treated nude mice were removed and frozen. Pure tumor cells were isolated from serial sections by laser capture microdissection and processed for microarray analyses. Approximately 60% of transcripts were co-expressed in the two microenvironments. However, subsets of genes were uniquely expressed in tumors or their LN metastases. Among transcripts upregulated in the LNs were ones encoding CD44. This was confirmed by immunohistochemical analyses from matched tumors, LV emboli, and LN metastases, which showed that CD44 protein was upregulated in LV and LN metastases. We hypothesize that CD44 selects primary tumor cells for lymphatic transit. To determine if gene regulation by estrogen is altered in the LN microenvironment compared to the primary tumor, we also determined how the gene expression profiles in each compartment changed when estradiol was removed. Interestingly, different subsets of genes were estrogen regulated in the LN compared to the primary tumor. These results suggest that therapeutics targeting ER+ breast cancers differentially affect primary tumors and their metastases. DOD grant to JCH BC050889.

Publications from the past 12 months

Estrogen Receptor Positive Breast Cancer Metastasis: Altered Hormonal Sensitivity and Tumor Aggressiveness in Lymphatic Vessels and Lymph Nodes

Joshua Chuck Harrell,^{1,3} Wendy W. Dye,¹ D. Craig Allred,⁴ Paul Jedlicka,² Nicole S. Spoelstra,¹ Carol A. Sartorius,¹ and Kathryn B. Horwitz^{1,2,3}

Departments of ¹Medicine, ²Pathology, and ³Program in Reproductive Sciences, University of Colorado Health Sciences Center, Aurora, Colorado; and ⁴Breast Center, Baylor College of Medicine, Houston, Texas

Abstract

Breast cancers commonly spread to lymph nodes (LNs). If the primary tumors are estrogen receptor (ER) and/or progesterone receptor (PR) positive, then the likelihood that LN metastases express receptors exceeds 80%. However, due to lack of ER+ models, little is known about the role of hormones in breast cancer spread or the effects of the LN microenvironment on hormone responsiveness. We have developed metastasis models using ZsGreen labeled MCF-7 and T47D human breast cancer cells. Tumors are tracked in living mice by whole-body imaging, and macrometastases or micrometastases are detected by intravital imaging or fluorescence microscopy. Tumor growth is estrogen dependent and required for intratumoral lymphangiogenesis. Seventy-five percent of all tumors and >95% of larger tumors generate LN metastases. Occasionally more distant metastases are also observed. "Triads" of primary tumors, tumor-filled draining lymphatic vessels, and tumor-filled LNs from the same mouse show that (a) proliferation, as measured by 5-bromo-2'-deoxyuridine uptake, is higher in the LN than in the primary tumor. (b) High ER levels are extensively down-regulated by estradiol in primary tumors. However, there is partial failure of ER down-regulation in LNs associated with (c) reduced PR expression. This suggests that ER are dysfunctional in the LN microenvironment and perhaps hormone resistant. (d) CD44 is sparsely expressed in primary tumor cells but homogeneously overexpressed in cells transiting the lymphatics and populating LNs. We hypothesize that CD44 expression targets tumor cells for transport to, and uptake in, LNs. If so, the CD44 pathway could be targeted therapeutically to slow or prevent LN metastases. (Cancer Res 2006; 66(18): 9308-15)

Introduction

Advanced breast cancer kills >40,000 American women each year and 10 times that number worldwide (1, 2). Seventy to 80% of primary breast cancers are estrogen receptor (ER) and/or progesterone receptor (PR) positive and considered to be hormone responsive (3). Importantly, if the primary tumors are ER+, >80% of lymph node (LN) metastases and 65% to 70% of distant metastases retain their receptors (4–6). Despite this, little is known about the role, if any, of estrogens or progestins in influencing the spread of

tumor cells from the primary site, or their deposition and growth at metastatic sites.

This lack of information is due, in part, to a lack of ER+ experimental metastasis models. The three ER+ human breast cancer cell lines most widely used for orthotopic xenograft studies are MCF-7, T47D, and ZR75 cells (7). They develop tumors in mammary glands of nude mice in response to estradiol supplementation (8, 9). However, most reports state that such tumors are poorly invasive and rarely, if ever, metastasize (9). Indeed, most metastasis models do not use these cells, relying instead on ER– cell lines like MDA-231, MDA-435 (10) and similar cells that express putative aggressiveness markers and do metastasize in nude mice. Other studies analyze only late stages of metastases by injecting ER– tumor cells directly into the circulation (11). Alternative approaches for studying tumor aggressiveness from orthotopic sites with ER+ breast cancer cells involve their modification to overexpress oncogenes like v-Ha-ras (12) or HER-2/neu (13), growth factors like vascular endothelial growth factor (14) or fibroblast growth factor (15), or transcription factors like Id-1 (16) or Fra-1 (17), in an effort to enhance tumor progression while suppressing estrogen-dependent behavior (18). We considered, however, that if the clinical data cited above are a guide, it should not be necessary to suppress hormone responsiveness to achieve a metastatic phenotype.

Observation of metastasis can be difficult, especially if few cells are involved or appropriate target organs are unexplored. The development of fluorescent proteins to genetically tag living cells has greatly increased the likelihood that metastases will be visualized (19). Indeed, jellyfish green fluorescent protein has been widely used for studies of ER– cells (20). Recently, a set of coral reef fluorescent proteins were identified that require no cofactors or substrates (21). These fluors have been modified to produce variants with even brighter fluorescence and enhanced emission characteristics than green fluorescent protein, and codon usage has been modified to optimize their mammalian expression. Among these fluors, ZsGreen has unique excitation and emission patterns within the visible spectrum.

This report reevaluates the metastatic potential of ER+ MCF-7 and T47D human breast cancer cells in orthotopic mouse tumors using ZsGreen as a sensitive new tracking method. Cells stably expressing this fluor and grown as xenografts in mammary glands of nude mice were absolutely estrogen dependent. Tumor fluorescence was stable and superficial LN metastases were monitored in living mice. At necropsy, stably fluorescent metastatic cells were reliably detected microscopically in lymphatics in local and distant LNs and, occasionally, in distant organs. If the primary tumors were ER+ and PR+, then metastases retained receptors, but their expression levels and that of the proliferation marker

Requests for reprints: Joshua Chuck Harrell, Department of Medicine/Endocrinology, University of Colorado Health Sciences Center, MS 8106, RC-1 South, Room 7402G, 12801 East 17th Avenue, P.O. Box 6511, Aurora, CO 80045. Phone: 303-724-3942; Fax: 303-724-3920; E-mail: joshua.harrell@uchsc.edu.

©2006 American Association for Cancer Research.
doi:10.1158/0008-5472.CAN-06-1769

5-bromo-2'-deoxyuridine (BrdUrd) were modified by the LN micro-environment. In addition, the hyaluronan receptors, CD44, which control chemotactic behavior of tumor cells (22), were up-regulated in cells transiting the lymphatics and retained in LNs. These data suggest strategies for suppressing LN metastases and indicate that once in the LNs, tumor cells have reduced hormonal sensitivity.

Materials and Methods

Cell lines. MCF-7 cells were originally purchased from American Type Culture Collection (Manassas, VA). Generation of T47D cells that express one PR isoform was previously described (23), and in the present study PR-B expressing T47D cells were used exclusively. The ZsGreen-N1 expression vector, PT-67 packaging cell line, and pLNCX2 retroviral vector were purchased from Clontech/Becton Dickinson (Franklin Lakes, NJ). Fluorescent retroviral vectors were generated by cloning the DNA coding sequence of ZsGreen into the pLNCX2 vector using the restriction enzymes *HindIII* and *NotI* and T4 ligase. Plasmids were then transfected into PT-67 packaging cells with a standard calcium phosphate protocol. Stable retrovirus producing cells were selected by 2 weeks of treatment with 500 $\mu\text{g}/\text{mL}$ G418. MCF-7 or T47D cells were plated at $\sim 20\%$ confluence and incubated in filtered, virus-containing supernatant. Cells were serially transduced two to three times for 24 hours each round, at which point they exhibited heterogeneous green expression. Cells were then subjected to G418 selection, followed by aseptic fluorescence associated cell sorting (FACS), to isolate a homogeneously bright green subpopulation. These cells were returned to culture and remained bright green through multiple passage generations. Expression of ER and PR in the selected cells was confirmed by immunohistochemistry (see below).

Xenograft tumor growth and metastases. All animal procedures were done under a protocol approved by the University of Colorado Institutional Animal Care and Use Committee. Ovariectomized female athymic *nu/nu* mice were obtained from Harlan Sprague-Dawley (Indianapolis, IN) at 5 to 6 weeks of age. To establish tumors, animals were anesthetized with Avertin and injected into the opening of the lactiferous duct of the abdominal mammary gland with 1 million ZsGreen-expressing MCF-7 or T47D cells in 100% Matrigel (Becton Dickinson). Mice were also implanted with silastic pellets containing cellulose (10 mg) or 17 β -estradiol (2 mg + 8 mg cellulose) as previously described (24). Tumor size was recorded weekly with a digital caliper. Fluorescent whole-body imaging was done weekly (Illumatool 9900, Lighttools Research, Encinitas, CA). Two hours before necropsy 100 mg/kg BrdUrd in PBS was injected i.p. At the end of the study, mice were euthanized by CO₂ asphyxiation and fluorescent intravital optical imaging was done by coupling the Illumatool with an Olympus (Melville, NY) SZ-61 dissecting microscope and Olympus C-5050 digital camera. Organs were removed for histology, immunohistochemistry, and fluorescence microscopy.

Histology, immunohistochemistry, and fluorescence microscopy. Organs were fixed in 4% paraformaldehyde overnight, paraffin embedded, and cut into 4- to 5- μm sections. After high-temperature antigen retrieval in citrate buffer, sections were stained with H&E. Immunohistochemistry was done on parallel sections for 1 hour at room temperature, with primary antibodies directed against ER (6F11; Vector Labs, Burlingame, CA), PR (1294; Dako, Carpinteria, CA), BrdUrd (Becton Dickinson), CK18 (Calbiochem, La Jolla, CA), CK8/CK18 (5D3; Novocastra, Newcastle-upon-Tyne, United Kingdom), LYVE-1 (Upstate, Lake Placid, NY), Prox-1 (Abcam, Cambridge, MA), or CD44 (Ab4; NeoMarkers/Labvision, Fremont, CA). Bound primary antibodies were detected with horseradish peroxidase (HRP)-conjugated goat anti-mouse and/or goat anti-rabbit secondary antibodies (Envision HRP; Dako). Sections were counterstained with hematoxylin and mounted. For immunofluorescence microscopy, goat anti-rabbit Alexa Fluor 555 (red) and goat anti-mouse Alexa Fluor 488 (green) secondary antibodies were used (Alexa Fluors; Invitrogen, Carlsbad, CA). For fluorescence microscopy, tissues were processed and sectioned as above, paraffin was removed with xylene, and then mounted with fluoromount G (EMS, Hatfield, PA).

Statistical analyses. Data from immunohistochemistry experiments were collected by an investigator who photographed tissue sections and a blinded

investigator that counted cells from random fields of stained sections using Image Pro software version 4.5.0.29 (Media Cybernetics, Inc., Silver Spring, MD). Each field was quantified either as a percentage of positively stained cells or an Allred score (ref. 25; percent of labeled cells added to the intensity of immunolabeling). Fields from the same tissue section were averaged and SPSS software version 12.0.2 (SPSS, Inc., Chicago, IL) was used to analyze the data. A Mann-Whitney *U* test was used to compare BrdUrd-positive HRP-stained cells in independent, nonparametric samples of estradiol- and placebo-treated mouse tumors. Paired *t* test was used to compare fluorescent-stained cells positive for CK18/BrdUrd, ER, or PR of tumor, LN, and associated lymphatic embolus triad from one mouse to those of other triads from other mice. A marginal homogeneity test was used to compare ER+ and PR+ HRP expression on Allred scores in nonparametric mouse triad samples. For all tests, $P < 0.05$ was considered significant.

Results

An *in vivo* model of estrogen-dependent human breast cancer LN metastasis. The ER+ human breast cancer cell lines MCF-7 and T47D are commonly used to study the biology of estrogen action *in vitro*. These cells also grow as estrogen-dependent xenografts in nude mice (8, 24, 26), but most published reports state that orthotopic tumors fail to metastasize. Because, clinically, ER+ tumors metastasize frequently (4–6), we decided to reevaluate the metastatic potential of ER+ human breast cancer cells in xenografts using sensitive new tracking methods. To this end, MCF-7 and T47D cells were retrovirally transduced with ZsGreen, G418 selected, and the brightest green subpopulation was isolated by FACS sorting. Confocal imaging showed that ZsGreen was highly expressed in both cell types, in the cytoplasm and nuclei (not shown). Intense fluorescence is maintained through multiple passages, the fluor is nontoxic, and photobleaching studies show that ZsGreen, a coral reef protein, is much brighter and more photostable than green fluorescent protein, a jellyfish protein (not shown).

Visualizing lymphovascular tumor cell spread. One million fluorescent tumor cells in Matrigel were injected into the lactiferous duct of the abdominal (#4) mammary gland of 5- to 6-week-old, ovariectomized *nu/nu* mice supplemented with an estradiol-releasing silastic pellet (24). This injection route led to formation of well-circumscribed tumor cell nodules distant from the subiliac LN in the gland, as shown by a whole mount 3 days after injection (Fig. 1A, *top*). In contrast, whole mount of a tumor at 12 weeks shows the subiliac LN, still physically distinct from the primary tumor but already highly involved with tumor cells (Fig. 1A, *bottom*).

This protocol was used to track the spread of ER+ tumors beyond the #4 mammary gland using whole-body imaging of live mice done weekly. Figure 1B shows an image of tumor tracks photographed through the skin of an intact mouse at 12 weeks. Bright green bilateral tumors are present in mammary gland #4 at the groin, and both subiliac mammary gland LNs contain tumor cells. Also clearly visible are tumor cell tracks in the epigastric collecting lymphatic vessels (LV) draining the tumor cranially on the right, as well as tumor cells in the right axillary LN. Similarly, three distinct green fluorescent clusters of tumor cells are faintly seen in the left lymphatics and axillary LN.

At sacrifice, intravital fluorescence microscopy was used to examine tumor spread to visceral tissues as shown in Fig. 1C and D. An axillary LN micrometastasis is seen in one mouse at 12 weeks (Fig. 1C, *left*) and a fully involved LN metastasis in another mouse at 12 weeks (Fig. 1C, *right*). Figure 1C also shows the afferent LV full of tumor cells, with the parallel epigastric vein devoid of such cells. Tumor cells also spread medially to the abdomen. Shown in Fig. 1D is early invasion into a periaortic LN

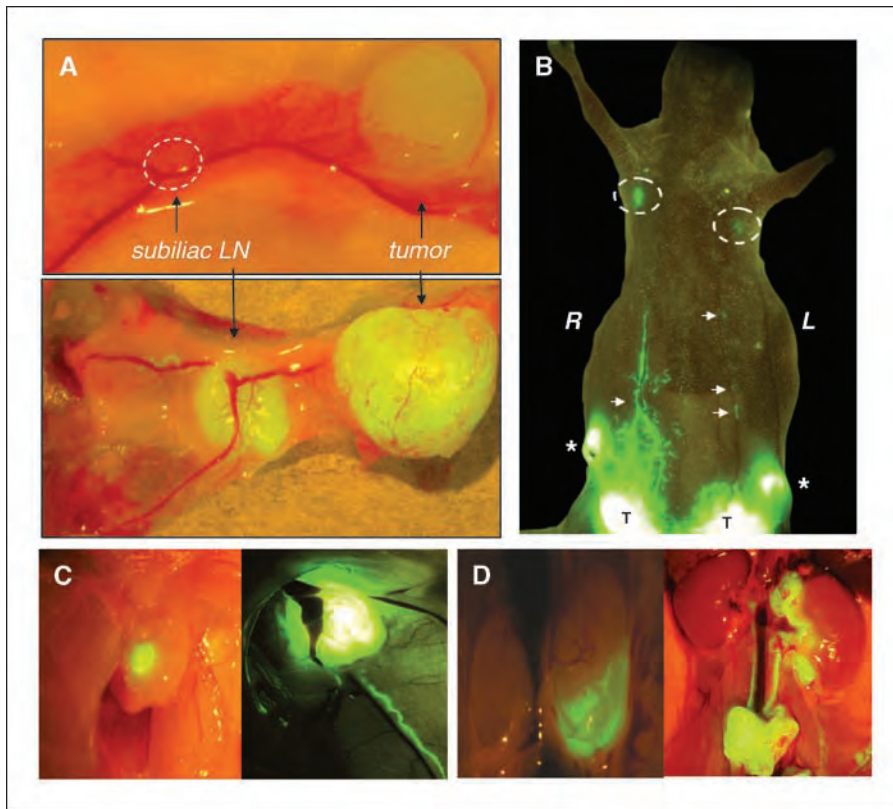


Figure 1. Whole-body and intravital images of ZsGreen-expressing ER+ human breast cancer cells and their LN metastases. *A*, excised abdominal mammary gland from a 3-day-old MCF-7 tumor, in relation to the subiliac LN (top, dashed circle), and from a 12-week-old MCF-7 tumor with a LN metastasis at a similar site (bottom). *B*, whole-body image showing bilateral T47D tumors (T), subiliac LN metastases (*), collecting LV (arrows), and axillary LN macrometastases (right) and micrometastases (left; dashed circles). *C*, intravital image of MCF-7 axillary LN metastasis showing a micrometastasis (left) and a macrometastasis (right) with a collecting LV draining into it. *D*, intravital image of an MCF-7 metastasis to the left para-aortic LN (left) and more progressive disease showing coalesced left and right para-aortic LNs and further tumor spread caudally to the renal LNs (right).

(left) and also much more extensive metastases to periaortic and renal LNs (right).

Bilateral tumor-filled lymphatic tracks exiting a primary tumor are clearly seen in Fig. 2A. LV full of tumor cells extend both cranially and medially from the tumor. It is possible that the tortuously branching network of lymphatics exiting the tumor cranially represents lymphangiogenesis. A higher-power view of the

laterally branching iliac LV shows that the tumor cells within it coalesced into emboli rather than moving as discrete cells. In response to mechanical pressure applied either to the tumor or the efferent lymphatic root during dissections, fluorescent emboli in collecting lymphatics can often be seen moving into their draining LN (not shown). This has implications for the order in which breast surgical procedures and sentinel node biopsies are done. In general,

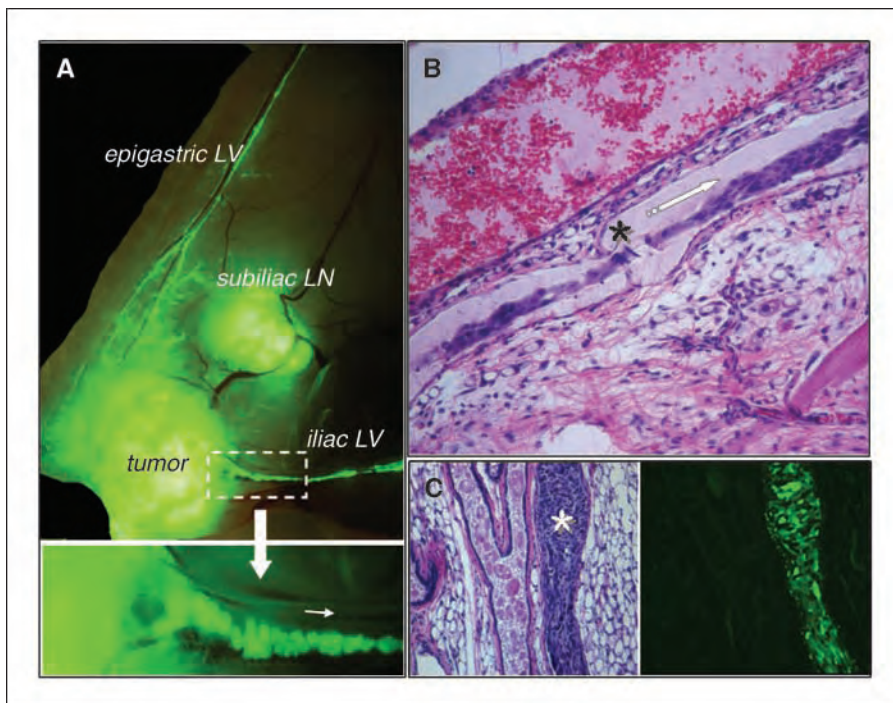


Figure 2. Identification of cancer cells in LVs. *A*, top, intravital image of a T47D tumor, showing its metastasis to the subiliac LN, and cells moving through the epigastric and iliac LVs. Bottom, higher magnification of the iliac LV showing clusters of cells moving inwards toward the para-aortic LNs. *B*, the isolated epigastric LV from (A) showing cancer cells moving through a collecting valve (*) in route to the axillary LN. *C*, left, an isolated collecting LV full of MCF-7 cancer cells (*) paralleling a milk duct. Right, a serial section confirms the identity of the cancer cells and shows maintenance of ZsGreen fluorescence after tissue processing into paraffin blocks.

tumor cell spread to the superficial LNs is restricted to the side of the body containing the primary tumor, and spread to deeper LNs becomes bilateral with progressive disease (Fig. 1D). Directional valves (*asterisk*) within the LV do not inhibit tumor cells moving through LVs, as shown in Fig. 2B. Lastly, fluorescence microscopy can be used to analyze clinicopathologic features of tumors and their metastases. Importantly, ZsGreen fluorescence is maintained throughout the histologic fixation process. Figure 2C shows the H&E stain of a collecting LV filled with tumor cells within the mammary gland fat pad. A milk duct runs alongside it. Fluorescence microscopy of a serial section confirms that tumor cells are restricted to the LV.

Estrogen-dependent tumor growth and rate of LN metastases. Figure 3 summarizes the primary tumor growth pattern of MCF-7 and T47D cells during 12 weeks of observation and the extent of LN metastasis as assessed by whole-body and intravital imaging. Growth from both cell types is estradiol dependent, with tumors nearly tripling in size in ~12 weeks (Fig. 3A). Both MCF-7 and T47D tumors produce LN metastases at the same rate, which increases with time and tumor size. At 2 weeks, no metastases occurred. By 4 weeks, ~14% of tumors generated LN metastases. This increased to ~75% at 12 weeks. Development of LN metastases seems to be size dependent (Fig. 3B). A separate time-course study of tumors grown for 1, 6, or 12 weeks showed that metastases to superficial subiliac and axillary LN, or to deeper visceral lateral iliac and aortic lumbar LN surrounding the aorta and kidneys, tend to occur at the same rate.

Estradiol and LV development. Because only estradiol-treated tumors yielded LN metastases, we next studied the effects of estradiol on tumor-associated LV development. For these studies, tumors were grown with or without estradiol supplementation for short term (3-10 days) or long term (6-12 weeks) and LV were quantified with lymphatic-specific LYVE-1 and Prox-1 (not shown) antibodies. Peritumoral LVs were identified in both treatment groups and likely represent lymphatics found adjacent to veins and arteries in the normal mouse mammary gland (Fig. 4). Intratumoral LVs were not seen after short-term estradiol treatment or in the estradiol-deprived dormant tumors. Fifty-eight percent of long-term estradiol-treated tumors contained intratumoral LVs (Fig. 4). ZsGreen fluorescence was quenched during the immunolabeling process, allowing for double immunostaining with anti-LYVE and anti-BrdUrd antibodies (Fig. 4) to assess the proliferation state of the LV. This procedure showed the LVs to be BrdUrd positive, suggesting that lymphangiogenesis was occurring. However, double labeling for LYVE and ER expression showed absence of ER in the LVs (not shown). We conclude that LV proliferation, although restricted to the estradiol-dependent growing tumors, is either not itself estradiol dependent or is occurring in response to paracrine signals from surrounding ER+ tumor cells.

The triad of primary tumor, lymphatic emboli, and LN metastases: proliferation. Our ability to dissect a primary tumor, its draining lymphatic collecting duct filled with tumor cells, and the downstream tumor-filled LN, from the same mouse, allows assessment of the role of the microenvironment in tumor cell proliferation and steroid receptor expression. BrdUrd uptake, measured with BrdUrd primary antibodies coupled to a HRP or a green fluorescent secondary antibody, was used to assess the proliferation rate of cells in these different compartments. In the absence of estradiol, tumor cells at the injection site remain viable and proliferate slowly with a labeling index <7% (Fig. 5A), but at a rate insufficient to elicit an overall increase in tumor

size at 12 (Fig. 3) or 16 to 20 weeks (not shown). These dormant tumors yield no LN metastases. In the presence of estradiol, primary tumors exhibit extensive BrdUrd uptake with a labeling index of ~20%.

To accurately quantify dispersed tumor cells and eliminate the contribution of proliferating normal host cells, tumor cells were immunolabeled with CK18 and a red secondary antibody. In this case, proliferating cells were quantified with anti-BrdUrd and a green fluorescent secondary antibody, and some sections were also counterstained with blue 4',6-diamidino-2-phenylindole (DAPI). Figure 5B shows two "triads" of tumor, LV and LN. Each triad came from the same mouse; the two sets were taken from two different mice. In triad 1, although the primary tumor cells have a high labeling index, proliferation in the LV embolus is low and mainly restricted to cells at the periphery, and in the LN, tumor cells are present only in the subcapsular sinus. The remainder consists of normal DAPI-stained LN cells (some of

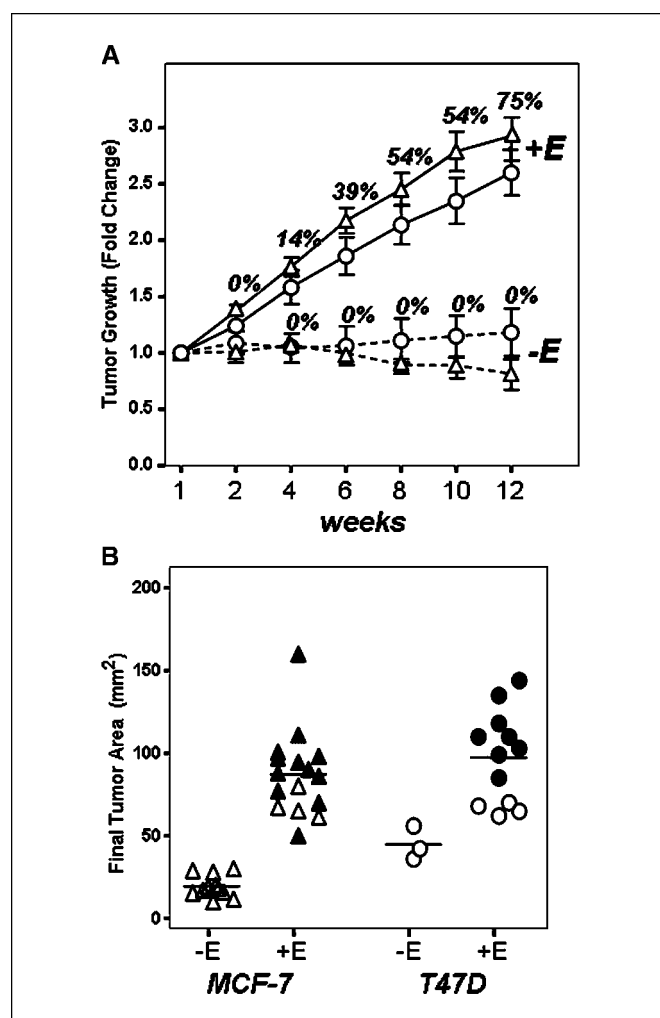


Figure 3. Estrogen-dependent tumor growth is required for LN metastasis. **A**, MCF-7 (triangles) and T47D (circles) tumors were grown either with (+E) or without (-E) estradiol for 12 weeks in ovariectomized nude mice. Tumor area was quantified with digital calipers and presence of metastases was assessed by weekly whole-body imaging and by intravital imaging at necropsy. The percent of mice with LN metastasis is indicated at each time point. **B**, tumor area at necropsy as assessed by the diameter in two dimensions. Filled symbols, tumors from which metastasis developed; open symbols, tumors that did not generate metastases.

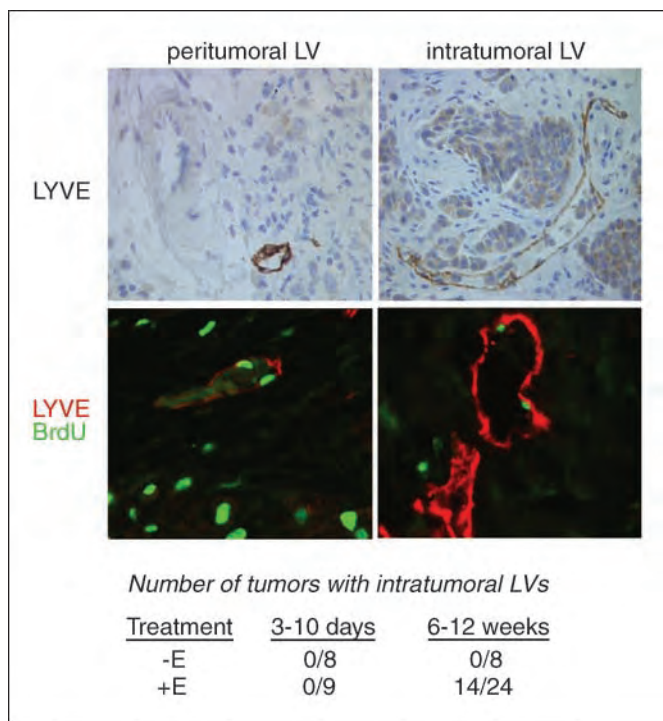


Figure 4. Assessment of tumor-associated lymphatics and lymphangiogenesis. Tumors from 3- to 10-day-old or 6- to 12-week-old placebo-treated (-E) and estradiol-treated (+E) ovariectomized mice were paraffin embedded. Top, sections (5 μm) were probed for LVs with an anti-LYVE-1 antibody and an HRP-labeled secondary antibody. Bottom, sections were probed by dual fluorescence immunohistochemistry with mouse anti-BrdUrd and rabbit anti-LYVE primary antibodies, followed by goat anti-mouse (green) and goat anti-rabbit (red) secondary antibodies, to identify lymphatics in S phase. The table quantifies the results.

which are also undergoing cell division). Triad 2 exhibits a different pattern, with extensive proliferation in the primary tumor and throughout the LV emboli, and the LN is highly involved with rapidly proliferating tumor cells.

Figure 5C quantifies all proliferation data. It shows, first, that the two methods of assessing BrdUrd uptake yielded similar results (compare the two +E "tumor" sets—one assessed with HRP and the other with dual BrdUrd/CK18 immunohistochemistry). As expected, compared with dormant controls, estradiol-treated primary tumors exhibit a statistically significant increase in proliferation rate from ~7 to ~20%. And, compared with the primary tumors, metastatic cells in the LN microenvironment have a statistically significant ($P = 0.003$) further increase to ~27%. Proliferation rates of embolic cells in the LV were variable and not statistically different from the other two compartments, although they tended to resemble those in the primary tumor more closely.

The triad of primary tumor, lymphatic emboli, and LN metastases: ER and PR. ER and PR immunohistochemistries for two sets of vehicle versus estradiol-treated triads using MCF-7 derived tumors show the heterogeneity observed (Fig. 6). In the absence of estradiol, levels of ER in tumors are always high. Estradiol treatment leads to extensive tumor ER down-regulation. ER tend to remain low in the LV and LN of Fig. 6 (top) but are somewhat restored in the LN of the second triad (bottom). No PR are expressed without estradiol induction. Estradiol treatment leads to heterogeneous PR expression in tumors, which tends to decrease in LV and LN of the same mouse. Quantitation of PR

data from several mice is shown in Fig. 6. There is a clear trend of decreased PR expression as cells spread into LV and LN ($P = 0.052$). A second experiment (not shown) using fluorescent immunohistochemistry for ER and PR showed a similar trend of reduced PR between five tumors and their matched LNs ($P = 0.09$). Each immunohistochemical procedure showed a

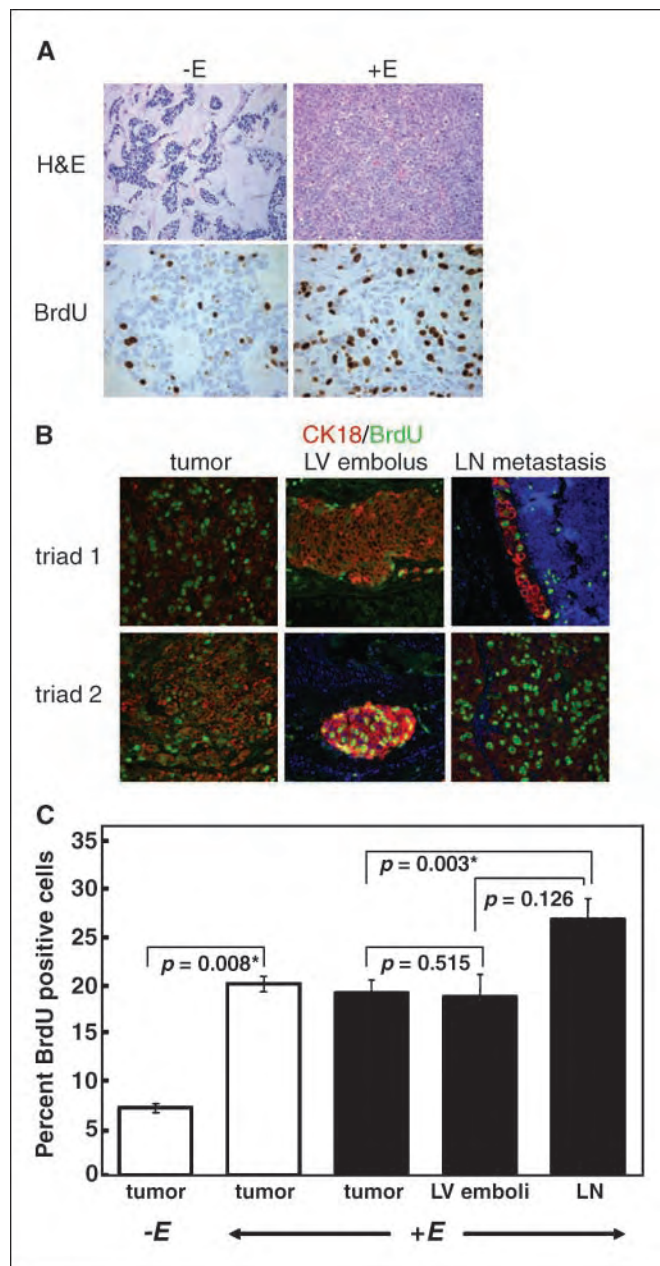


Figure 5. Assessment of tumor proliferation in MCF-7 tumors, LV emboli, and LN metastases. A, ovariectomized mice bearing MCF-7 tumors were treated for 12 weeks with placebo (-E) or estradiol (+E). Tumors were paraffin embedded, sectioned, and stained with H&E or analyzed by BrdUrd-HRP immunohistochemistry. B, dual fluorescence immunohistochemistry for cytokeratin 18 (red) and BrdUrd (green) of estradiol-treated MCF-7 tumors, LV emboli, and LN metastases. Each triad was taken from the same mouse. Anti-rabbit CK18 and anti-mouse BrdUrd primary antibodies and goat anti-rabbit (red) and goat anti-mouse (green) antibodies were used. A DAPI counterstain (blue) was occasionally included. The centrally necrotic regions of tumors were excluded from analyses. C, quantification of A and B ($n = 5$ for tumors and LNs; $n = 3$ for LVs), showing the data obtained from the HRP based protocol in A (white columns) and the dual CK18/BrdUrd protocol in B (black columns).

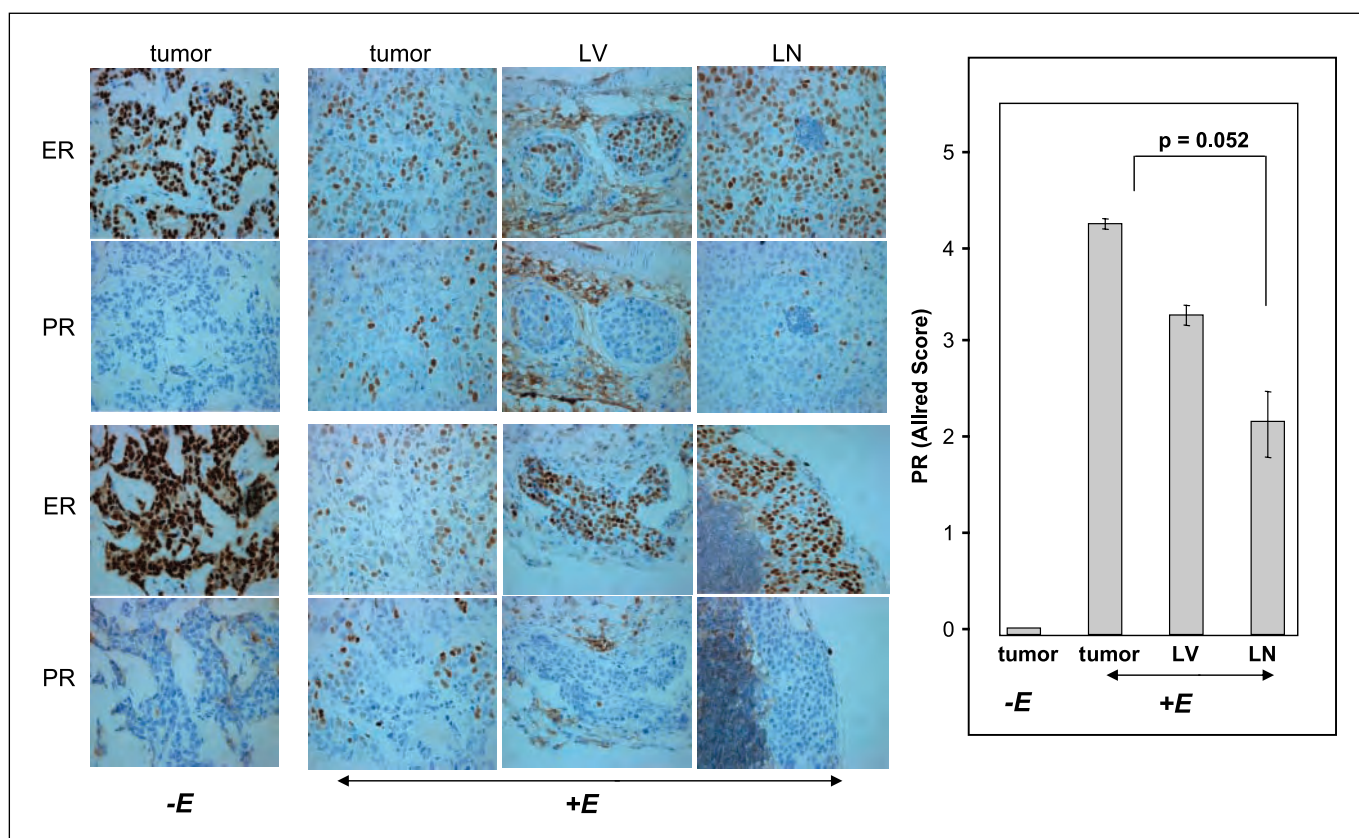


Figure 6. ER and PR expression in triads of MCF-7 tumors, LV emboli, and LN metastases. *Left*, representative images of two tumors from placebo ($-E$) treated mice and of two matched triads of estradiol-treated ($+E$) mice, showing tumors, their lymphatic emboli, and LN metastases. Paraffin-embedded sections were probed with mouse anti-ER or mouse anti-PR primary antibodies, coupled with goat anti-mouse HRP-conjugated secondary antibodies. *Right*, quantification of PR expression in placebo-treated ($n = 3$) and estradiol-treated tumors ($n = 7$), LV emboli ($n = 3$), and LN metastases ($n = 5$), based on the intensity of cellular staining combined with the percent of positive cells.

nonsignificant slight increase in ER expression in the LN metastases compared with the down-regulated ER in the estradiol-treated primary tumor.

Selection of cells for lymphatic transit: CD44. Hyaluronan regulates various aspects of cell behavior, particularly cell migration and invasiveness. It does so by binding to specific receptors on the cell surface, the best characterized of which is CD44 (22). Human breast cancer cells migrate directionally in response to a hyaluronan gradient depending on CD44 expression levels (22). Breast cancers secrete factors that up-regulate hyaluronan expression in osteoblasts (27), which may promote bone metastasis. Figure 7A shows CD44 expression levels in two primary tumors and in their LV and/or LN metastases. Set A (*top*) clearly shows extensive overexpression of CD44 in tumor cells occupying the LN microenvironment, compared with the same tumor cells in the mammary gland, where CD44 expression is sparse and heterogeneous. Set B includes a matched LV embolus and again shows sparse and heterogeneous CD44 in the tumor, but homogenous and elevated CD44 in both the LV embolic tumor cells, and the LN metastases.

Distant metastases. Metastases to distant organs were occasionally observed with these models. Figure 7B (*left*) shows H&E staining of tumor cells metastatic to the lung. Their identity is confirmed by intense ZsGreen fluorescence in a serial section (Fig. 7B, *right*). These lung metastases could have arisen by direct peritumoral venous invasion and spread (the most direct route to

the lungs from distant body sites) or they may reflect indirect spread from an overwhelmed lymphatic system via lymphatic-venous anastomoses. Both mechanisms may contribute to distant organ metastasis in humans (28). It should be stressed that these metastases were rare and they occurred only in animals that also had extensive LN spread.

Perineurial invasion. Perineurial invasion was also noted in tumors arising from both cell lines. Perineurial invasion is observed in a variety of human carcinomas and may contribute to local-regional tumor spread, although it has not been shown to be an independent prognostic indicator in human mammary carcinomas (29). Although not as frequent as lymphatic invasion, perineurial invasion was occasionally found at tumor margins and along the peripheral nerves that parallel the iliac veins. Figure 7C shows an H&E stain (*left*) and CK18 immunohistochemistry (*right*) of T47D tumor cells (*arrow*) tracking along a peripheral nerve (*asterisk*).

Discussion

LN metastasis in association with tumor size is the single most powerful indicator of poor prognosis in mammary carcinoma (30, 31). Pathologic data sets of patients with breast cancer indicate that, at diagnosis, presence of tumor-infiltrated LNs is common, with estimates ranging from 30% to 50% of cases (32–34), depending on tumor size. The dominant feature of the present model is rapid and reliable LN metastasis of ER+ cells

from orthotopic tumor sites. Two different cell lines, MCF-7 and T47D, generated estrogen-dependent solid tumors and reliably produced metastases to local and distant LNs. Under conditions of the studies, which were terminated at 12 weeks, tumor cells in LV and LN metastases were observed in 75% of all mice and in essentially 100% of mice, the primary tumors of which exceeded $\sim 75 \text{ mm}^2$ in area (Fig. 3). Clinically, the association between tumor size and LN involvement is well known (35). Metastases to other sites, like the lungs (Fig. 7B), were occasionally observed, as were cells migrating along peripheral nerve tracks (Fig. 7C). The ability of the latter routes to reliably colonize distant organs undoubtedly will require longer observation times. This is suggested by the studies of others. Half a million ER⁻ MDA-231 breast cancer cells, injected directly into the circulation, nevertheless required 10 to 12 weeks before exhibiting limb bone metastases in 30% of mice (36). ER⁺ ZR75 cells injected into the circulation of mice required 3 to 6 months to yield similar bone metastases (37).

Use of modified breast cancer cells overexpressing hormones (38), growth factors (14, 39), and oncogenes (12) shows that the

metastatic potential, route of dispersal, time to metastasis, and preferred organ arrest site of any cell line are dependent on unique factors elaborated by that cell, and that much remains to be learned about the role of estrogens and progestins on these processes. For example, it has been reported that clinically, ER⁺ tumors are more likely to spread to bones whereas ER⁻ tumors more commonly metastasize to the viscera (40, 41). ER⁺ metastasis models, reflecting the clinical situation, could help define molecular mechanisms involved in such tissue specificity.

Expression profiling of matched primary and metastatic LN tumor pairs in clinical samples has failed to identify genes that distinguish one from the other (42) because metastases are genetically more closely related to the primary tumor from which they arose than to any other metastasis. However, within matched pairs, select genes are differentially expressed between the tumor and LN metastasis. Common among these are extracellular matrix and cell-matrix interacting genes, like the hyaluronan receptor CD44, which mediates rolling, attachment, and migration of cells on a hyaluronan substratum (43, 44). We show here that CD44 is sparsely and heterogeneously expressed in primary tumors but homogeneously overexpressed in LV tumor cell emboli and LN metastases (Fig. 7). Because directional migration of breast cancer cells towards hyaluronan is dependent on CD44 (22), we propose that the CD44⁺ subpopulation of primary tumor cells is preferentially propelled into tumoral lymphatics, and from there to LNs. If so, therapeutic targeting of the CD44⁺ subpopulation in a primary tumor could prevent LN metastases.

There is a high concordance rate ($\sim 80\text{-}90\%$) in ER expression between primary tumors and matched LN metastases (5). However, in the same patient, considerable disparities can exist in the concentrations of ER at the two sites, with ER levels often (6, 45) but not always (45) higher in the LN than in the local primary tumor. We observe a pattern (Fig. 6) in which ER levels are higher in the LN than in the primary tumor of the same mouse, an indicator of ER down-regulation failure in the LN microenvironment. It has been reported that there is an association between estrogen-dependent ER down-regulation and improved transcriptional efficacy of the receptors (46). Although it might be counterintuitive to think that in the presence of estrogen, lower ER levels signal a stronger hormone response, this seems to be the case. Thus, the inefficient ER down-regulation in the LN could be associated with poorer hormone responsiveness at that site. In the mouse tumors, PR expression levels (Fig. 6), which are markers of estrogen action and ER function, support this hypothesis. Assessment of PR levels in LNs and matched primary tumors shows a trend towards a decrease in LN PR (Fig. 6). This would be predicted by inefficient ER down-regulation. Clinically, both up-regulation and down-regulation of PR have been reported in the LN compared with primary tumors (45), but this has not been correlated to ER in the same samples.

We also observe a statistically significant increase in the proliferation rate of LN metastases compared with matched primary tumors (Fig. 5B and C). Clinically, increased mitoses in nodal metastases compared with primary tumors have been reported (47), possibly due to release of cytokines and growth factors, such as insulin-like growth factor-I and epidermal growth factor, by the LN (48). The implications of this growth promotion within LNs for failure of hormone treatments in metastatic disease could be important. If, in the LN microenvironment, cytokines and growth factors are the dominant mitogens, then LN metastases would be less sensitive than primary tumors to estradiol-suppressive therapies. Indeed, in metastatic disease,

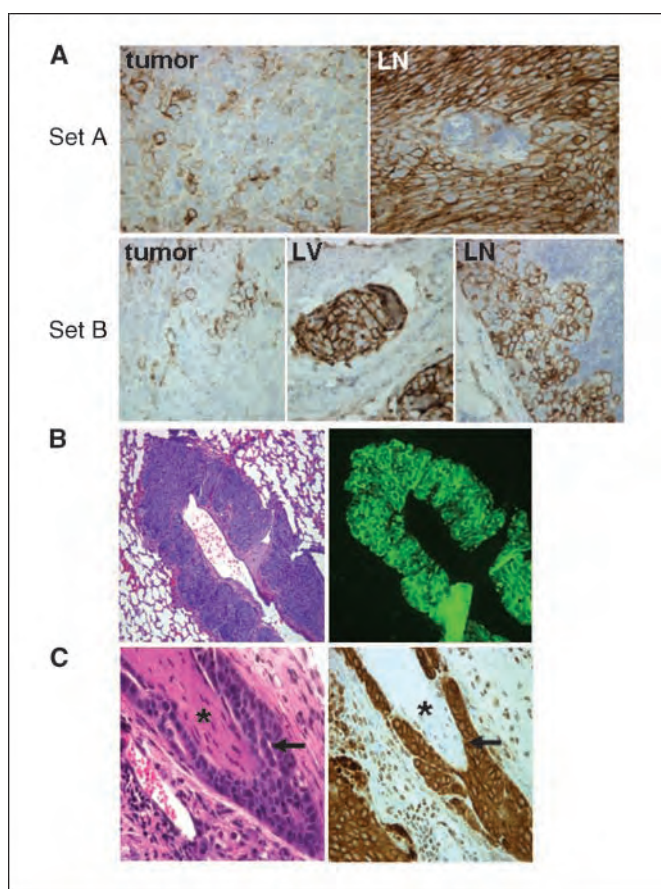


Figure 7. Selection of CD44⁺ MCF-7 tumor cells for lymphatic transit and examples of lung metastases and perineurial invasion. *A*, tumors ($n = 5$) taken from estradiol-treated mice, and their matched LV ($n = 3$) and/or LNs ($n = 6$), were probed with mouse anti-CD44 and goat anti-mouse HRP-conjugated secondary antibodies. *Top*, a tumor and its matching LN. *Bottom*, a triad of tumor, LV, and LN taken from the same mouse. *B*, *left*, H&E stain of a paraffin-embedded section of T47D cells from an estradiol-treated mouse with metastasis to the lung. *Right*, a serial section processed for fluorescence microscopy. *C*, *left*, H&E stain of MCF-7 tumor cells from an estradiol-treated mouse showing perineurial invasion. *Right*, CK18 stain of a deeper section. *, nerve; arrow, tumor cells.

tamoxifen, which targets ER signaling pathways, is rarely associated with long-term remission, exhibiting decreased mean time to disease progression and decreased duration of response than local disease (41, 49, 50).

In summary, we have developed models of ER+ human breast cancers that reliably spread to LNs from solid tumors. Through the use of a new generation fluorescent protein, ZsGreen, we are able to identify cancer cells in tumors, LV emboli, LNs, and, occasionally, more distant sites for further molecular analysis. These studies show that the tumor cells found in LNs overexpress markers associated with tumor aggressiveness. At the same time, the LN microenvironment may suppress estrogen sensitivity of tumor

cells, which would make them more resistant than primary tumors to ER-targeted treatments.

Acknowledgments

Received 5/16/2006; revised 7/6/2006; accepted 7/25/2006.

Grant support: Department of Defense Predoctoral Breast Cancer Training Grant BC050889 (J.C. Harrell); Susan G. Komen Breast Cancer Foundation BCTR0402682 (C.A. Sartorius); and NIH grant CA26869, National Foundation for Cancer Research, the Avon Foundation, and the Breast Cancer Research Foundation grants (K.B. Horwitz).

The costs of publication of this article were defrayed in part by the payment of page charges. This article must therefore be hereby marked *advertisement* in accordance with 18 U.S.C. Section 1734 solely to indicate this fact.

We thank the University of Colorado Cancer Center Flow Cytometry and Sequencing Core Laboratories.

References

- Hayes DF, Isaacs C, Stearns V. Prognostic factors in breast cancer: current and new predictors of metastasis. *J Mammary Gland Biol Neoplasia* 2001;6:375–92.
- Parkin DM, Bray F, Ferlay J, Pisani P. Global cancer statistics, 2002. *CA Cancer J Clin* 2005;55:74–108.
- Keen JC, Davidson NE. The biology of breast carcinoma. *Cancer* 2003;97:825–33.
- Zheng WQ, Lu J, Zheng JM, Hu FX, Ni CR. Variation of ER status between primary and metastatic breast cancer and relationship to p53 expression. *Steroids* 2001;66:905–10.
- Butler JA, Trezona T, Vargas H, State D. Value of measuring hormone receptor levels of regional metastatic carcinoma of the breast. *Arch Surg* 1989;124:1131–4; discussion 4–5.
- Hoehn JL, Plotka ED, Dickson KB. Comparison of estrogen receptor levels in primary and regional metastatic carcinoma of the breast. *Ann Surg* 1979;190:69–71.
- Clarke R. Human breast cancer cell line xenografts as models of breast cancer. The immunobiologies of recipient mice and the characteristics of several tumorigenic cell lines. *Breast Cancer Res Treat* 1996;39:69–86.
- Osborne CK, Hobbs K, Clark GM. Effect of estrogens and antiestrogens on growth of human breast cancer cells in athymic nude mice. *Cancer Res* 1985;45:584–90.
- Lacroix M, Leclercq G. Relevance of breast cancer cell lines as models for breast tumours: an update. *Breast Cancer Res Treat* 2004;83:249–89.
- Mukhopadhyay R, Theriault RL, Price JE. Increased levels of $\alpha 6$ integrins are associated with the metastatic phenotype of human breast cancer cells. *Clin Exp Metastasis* 1999;17:325–32.
- Yoneda T, Williams PJ, Hiraga T, Niewolna M, Nishimura R. A bone-seeking clone exhibits different biological properties from the MDA-MB-231 parental human breast cancer cells and a brain-seeking clone *in vivo* and *in vitro*. *J Bone Miner Res* 2001;16:1486–95.
- Dickson RB, Kasid A, Huff KK, et al. Activation of growth factor secretion in tumorigenic states of breast cancer induced by 17 β -estradiol or v-Ha-ras oncogene. *Proc Natl Acad Sci U S A* 1987;84:837–41.
- Benz CC, Scott GK, Sarup JC, et al. Estrogen-dependent, tamoxifen-resistant tumorigenic growth of MCF-7 cells transfected with HER2/neu. *Breast Cancer Res Treat* 1993;24:85–95.
- Mattila MM, Ruohola JK, Karpanen T, Jackson DG, Alitalo K, Harkonen PL. VEGF-C induced lymphangiogenesis is associated with lymph node metastasis in orthotopic MCF-7 tumors. *Int J Cancer* 2002;98:946–51.
- McLeskey SW, Zhang L, Kharbanda S, et al. Fibroblast growth factor overexpressing breast carcinoma cells as models of angiogenesis and metastasis. *Breast Cancer Res Treat* 1996;39:103–17.
- Lin CQ, Singh J, Murata K, et al. A role for Id-1 in the aggressive phenotype and steroid hormone response of human breast cancer cells. *Cancer Res* 2000;60:1332–40.
- Belguise K, Kersual N, Galtier F, Chalbos D. FRA-1 expression level regulates proliferation and invasiveness of breast cancer cells. *Oncogene* 2005;24:1434–44.
- Thompson EW, Brunner N, Torri J, et al. The invasive and metastatic properties of hormone-independent but hormone-responsive variants of MCF-7 human breast cancer cells. *Clin Exp Metastasis* 1993;11:15–26.
- Hoffman RM. The multiple uses of fluorescent proteins to visualize cancer *in vivo*. *Nat Rev Cancer* 2005;5:796–806.
- Kim LS, Huang S, Lu W, Lev DC, Price JE. Vascular endothelial growth factor expression promotes the growth of breast cancer brain metastases in nude mice. *Clin Exp Metastasis* 2004;21:107–18.
- Richards B, Zharkikh L, Hsu F, Dunn C, Kamb A, Teng DH. Stable expression of Anthozoa fluorescent proteins in mammalian cells. *Cytometry* 2002;48:106–12.
- Tzircotis G, Thorne RF, Isacke CM. Chemotaxis towards hyaluronan is dependent on CD44 expression and modulated by cell type variation in CD44-hyaluronan binding. *J Cell Sci* 2005;118:5119–28.
- Sartorius CA, Groshong SD, Miller LA, et al. New T47D breast cancer cell lines for the independent study of progesterone B- and A-receptors: only anti-progestin-occupied B-receptors are switched to transcriptional agonists by cAMP. *Cancer Res* 1994;54:3868–77.
- Sartorius CA, Shen T, Horwitz KB. Progesterone receptors A and B differentially affect the growth of estrogen-dependent human breast tumor xenografts. *Breast Cancer Res Treat* 2003;79:287–99.
- Harvey JM, Clark GM, Osborne CK, Allred DC. Estrogen receptor status by immunohistochemistry is superior to the ligand-binding assay for predicting response to adjuvant endocrine therapy in breast cancer. *J Clin Oncol* 1999;17:1474–81.
- Shafie SM, Grantham FH. Role of hormones in the growth and regression of human breast cancer cells (MCF-7) transplanted into athymic nude mice. *J Natl Cancer Inst* 1981;67:51–6.
- Bose N, Masellis AM. Secretory products of breast cancer cells up-regulate hyaluronan production in a human osteoblast cell line. *Clin Exp Metastasis*. In press 2006.
- Kuman V, Fausto N, Abbas A, editors. *Robbins and Cotran pathologic basis of disease*. 7th ed. Philadelphia: Elsevier; 2004.
- Mills SE, Carter D, Greenson JK, Oberman HA, Reuter V, Stoler MH, editors. *Sternberg's diagnostic surgical pathology*. 4th ed. Philadelphia: Lippincott, Williams and Wilkins; 2003.
- McGuire WL. Prognostic factors for recurrence and survival in human breast cancer. *Breast Cancer Res Treat* 1987;10:5–9.
- Foster RS, Jr. The biologic and clinical significance of lymphatic metastases in breast cancer. *Surg Oncol Clin N Am* 1996;5:79–104.
- Vinh-Hung V, Verschraegen C, Promish DI, et al. Ratios of involved nodes in early breast cancer. *Breast Cancer Res* 2004;6:R680–8.
- Veronesi U, Paganelli G, Viale G, et al. Sentinel lymph node biopsy and axillary dissection in breast cancer: results in a large series. *J Natl Cancer Inst* 1999;91:368–73.
- Jatoi I, Hilsenbeck SG, Clark GM, Osborne CK. Significance of axillary lymph node metastasis in primary breast cancer. *J Clin Oncol* 1999;17:2334–40.
- Carter CL, Allen C, Henson DE. Relation of tumor size, lymph node status, and survival in 24,740 breast cancer cases. *Cancer* 1989;63:181–7.
- Kang Y, Siegel PM, Shu W, et al. A multigenic program mediating breast cancer metastasis to bone. *Cancer Cell* 2003;3:537–49.
- Guise TA, Yin JJ, Mohammad KS. Role of endothelin-1 in osteoblastic bone metastases. *Cancer* 2003;97:779–84.
- Guise TA, Yin JJ, Thomas RJ, Dallas M, Cui Y, Gillespie MT. Parathyroid hormone-related protein (PTHrP)-(1-139) isoform is efficiently secreted *in vitro* and enhances breast cancer metastasis to bone *in vivo*. *Bone* 2002;30:670–6.
- Padera TP, Kadambi A, di Tomaso E, et al. Lymphatic metastasis in the absence of functional intratumor lymphatics. *Science* 2002;296:1883–6.
- Koenders PG, Beex LV, Langens R, Kloppenborg PW, Smals AG, Benraad TJ. Steroid hormone receptor activity of primary human breast cancer and pattern of first metastasis. The Breast Cancer Study Group. *Breast Cancer Res Treat* 1991;18:27–32.
- Fuqua SA. The role of estrogen receptors in breast cancer metastasis. *J Mammary Gland Biol Neoplasia* 2001;6:407–17.
- Weigelt B, Wessels LF, Bosma AJ, et al. No common denominator for breast cancer lymph node metastasis. *Br J Cancer* 2005;93:924–32.
- Toole BP. Hyaluronan: from extracellular glue to pericellular cue. *Nat Rev Cancer* 2004;4:528–39.
- Clark RA, Alon R, Springer TA. CD44 and hyaluronan-dependent rolling interactions of lymphocytes on tonsillar stroma. *J Cell Biol* 1996;134:1075–87.
- De la Haba-Rodriguez JR, Ruiz Borrego M, Gomez Espana A, et al. Comparative study of the immunohistochemical phenotype in breast cancer and its lymph node metastatic location. *Cancer Invest* 2004;22:219–24.
- Lonard DM, Nawaz Z, Smith CL, O'Malley BW. The 26S proteasome is required for estrogen receptor- α and coactivator turnover and for efficient estrogen receptor- α transactivation. *Mol Cell* 2000;5:939–48.
- Hasebe T, Konishi M, Iwasaki M, et al. Histological characteristics of tumor cells and stromal cells in vessels and lymph nodes are important prognostic parameters of extrahepatic bile duct carcinoma: a prospective study. *Hum Pathol* 2005;36:655–64.
- LeBede C, Chen K, Fallavollita L, Boutros T, Brodt P. Peripheral lymph node stromal cells can promote growth and tumorigenicity of breast carcinoma cells through the release of IGF-1 and EGF. *Int J Cancer* 2002;100:2–8.
- Rose C, Mouridsen HT. Treatment of advanced breast cancer with tamoxifen. *Recent Results Cancer Res* 1984;91:230–42.
- Bratherton DG, Brown CH, Buchanan R, et al. A comparison of two doses of tamoxifen (Nolvadex) in postmenopausal women with advanced breast cancer: 10 mg bd versus 20 mg bd. *Br J Cancer* 1984;50:199–205.

Spontaneous Fusion with, and Transformation of Mouse Stroma by, Malignant Human Breast Cancer Epithelium

Britta M. Jacobsen,^{1,3} J. Chuck Harrell,¹ Paul Jedlicka,² Virginia F. Borges,^{1,4} Marileila Varella-Garcia,^{1,4} and Kathryn B. Horwitz^{1,2,3}

Departments of ¹Medicine and ²Pathology, Divisions of ³Endocrinology and ⁴Oncology, University of Colorado at Denver and Health Sciences Center, Aurora, Colorado

Abstract

Adenocarcinoma cells from the pleural effusion of a patient with breast cancer were injected into the mammary glands of nude mice and grown into solid tumors. A cell line derived from these tumors expressed α -smooth muscle actin but not human cytokeratin 7, indicating “activated” stroma of mouse origin. Cells in mitosis exhibited mainly polyploid mouse karyotypes, but 30% had mixed mouse and human chromosomes, among which 8% carried mouse/human translocations. Nuclei of interphase cells were 64% hybrid. Hybrid mouse/human nuclei were also detected in the primary xenograft. Thus, synkaryons formed in the solid tumor by spontaneous fusion between the malignant human epithelium and the surrounding normal host mouse stroma. The transformed stroma-derived cells are tumorigenic with histopathologic features of malignancy, suggesting a new mechanism for tumor progression. (Cancer Res 2006; 66(16): 8274-9)

Introduction

The epithelial cell subpopulation and its genetic alterations have traditionally driven our understanding of the biology and metastatic behavior of adenocarcinomas (1). Recently, however, studies have focused on the stromal microenvironment at the tumor boundary and its possible role in tumor progression (1). Stromal “activation” or desmoplasia is observed in many human malignancies including breast cancers (2–4). It has been defined as stroma that exhibits reactivation of fetal-like phenotypic properties with reexpression of cytokines, growth factors, and their receptors; changes resembling ones normally observed in wound healing (5). In malignancies, such changes contribute to altered epithelial cell morphology, accelerated cell migration, extracellular matrix remodeling, and angiogenesis (1, 6, 7).

Whether “activated” stroma is genetically transformed has been under debate. Multiple studies report that stromal enzymes and growth factors, although reexpressed in malignancies (8–11), are not otherwise different from normal patterns observed during

nonneoplastic tissue remodeling (10). Therefore, it has been proposed that epigenetic mechanisms are involved in these changes (1, 4, 12). However, some recent studies have reported the loss of heterozygosity in DNA isolated from microdissected tumor stroma, with changes that are either similar to (13, 14) or distinct from (14, 15) the genetic modifications found in the adjacent malignant epithelium. This would suggest genetic mechanisms for stromal remodeling. Tumor-associated vascular endothelial cells with cytogenetic abnormalities have also been reported (16), and both benign (e.g., fibroadenoma) and malignant (e.g., metaplastic carcinomas and sarcoma phyllodes) tumors are known to arise in, or resemble breast stroma (17). These studies also suggest the possibility that juxtatumoral stroma can be genetically different from normal stroma. However, the mechanisms for such genetic changes remain unclear. One proposal posits that carcinogenic events that alter the epithelium simultaneously alter the stroma (1, 15). Another proposes that cell-cell fusion, with generation of hybrid variants, can contribute to tumor cell diversity (18). We now report direct evidence using an experimental model system, for the malignant transformation of normal host stroma induced by fusion with malignant epithelium. The hybrid cells thus generated are capable of forming highly aggressive tumors.

Materials and Methods

Pleural effusion and cell culture. The patient, a 65-year-old female, presented with a 3 cm, poorly differentiated infiltrating ductal carcinoma with involved lymph nodes. The tumor was estrogen receptor (ER)-positive, progesterone receptor (PR) unknown, HER2 unknown. After surgery, she received six cycles of Cytoxan, Adriamycin, and 5-fluorouracil, followed by radiation therapy and 5 years of Tamoxifen. Three years after completing Tamoxifen therapy, the patient presented with a malignant pleural effusion and underwent thoracentesis. Immunohistochemistry of the pleural cells showed them to be ER (0%), PR (7%), and HER2 (0%). An Institutional Review Board–approved tissue acquisition protocol and patient-informed consent were obtained to acquire blood and tissue for research purposes.

Immunocytochemistry. Cells were fixed and stained as previously described (19). Cells were stained with anti- α -smooth muscle actin (Novacastra, United Kingdom), or anti-cytokeratin 7 (DAKO, Carpinteria, CA). HeLa human cervical carcinoma cells served as controls. Nuclei were counterstained with 4',6'-diamidino-2-phenylindole (DAPI).

Immunohistochemistry. Tumors were excised and processed as previously described (19). Five-micrometer sections were cut, fixed, and stained as described. Immunohistochemistry for ER used the monoclonal antibody 1D5 (DAKO).

Xenografts: BC6 cells and creation of BJ3Z cell line. Pleural effusion cells were passaged once *in vitro* in the presence of penicillin/streptomycin for 72 hours to remove debris. Four million adherent or floating cells (named BC6 cells) in 100% Matrigel (BD Biosciences/Clontech, Mountain View, CA) were separately xenografted into each fourth mammary gland of ovariectomized *nu/nu* mice, supplemented with a 17 β -estradiol (E)

Note: Supplementary data for this article are available at Cancer Research Online (<http://cancerres.aacrjournals.org/>).

K.B. Horwitz, B.M. Jacobsen, M. Varella-Garcia, and J.C. Harrell designed the research; J.C. Harrell, M. Varella-Garcia, and B.M. Jacobsen performed the research; V.F. Borges contributed the BC6 breast cancer cells; B.M. Jacobsen, M. Varella-Garcia, J.C. Harrell, and P. Jedlicka analyzed the data; K.B. Horwitz and B.M. Jacobsen wrote the paper.

Requests for reprints: Britta M. Jacobsen, Department of Medicine/Endocrinology, University of Colorado School of Medicine, Mail Stop 8106, P.O. Box 6511, Aurora, CO 80045. Phone: 303-724-3942; Fax: 303-724-3920; E-mail: Britta.Jacobsen@uchsc.edu.

©2006 American Association for Cancer Research.
doi:10.1158/0008-5472.CAN-06-1456

releasing pellet to yield circulating hormone levels of 145 ± 47 pg/mL, and grown into tumors for 12 weeks. One tumor was excised, and a representative portion was fixed, paraffin embedded, sectioned ($5 \mu\text{m}$), and stained with H&E. Cells in the remaining tumor segment were dispersed without enzymes using a pestle and $45 \mu\text{m}$ nylon mesh, and cultured in 10% FCS containing MEM (20). A permanent cell line, BJZ3, was established.

Fluorescent BJZ3 cells. BJZ3 cells were transduced with ZsGreen expressing viruses and highly green fluorescent cells were isolated by flow cytometry to yield "BJZ3g" cells. One million cells were injected bilaterally into the fourth mammary gland of ovariectomized nude mice and tumor size was measured biweekly for 11 weeks. Fluorescent intravital imaging used an Olympus (Melville, NY) SZ-61 dissecting microscope coupled to an Olympus C-5050 digital camera, under white light or a 470 nm excitation filter and 515 nm viewing filter incorporated into the imaging equipment. Fluorescence imaging of BJ12 histologic ($5 \mu\text{m}$) sections were done using a Nikon (Melville, NY) Eclipse E600 microscope with 480/30 nm excitation and 535/40 nm emission filters at $200\times$ magnification.

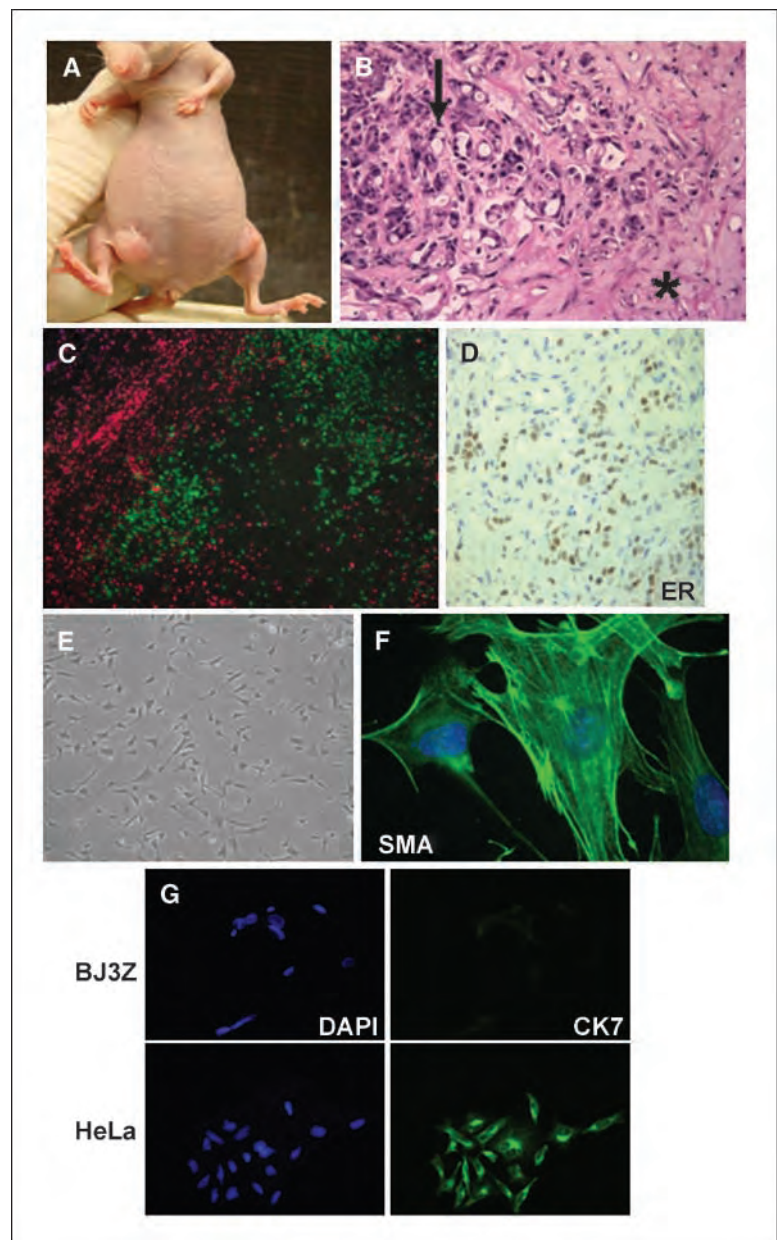
Karyotyping and fluorescence *in situ* hybridization. Cells in the log phase of growth were fixed and labeled as previously described (21). Metaphase spreads from BJZ3 cells were hybridized with human or mouse Cot-1 DNA labeled with SpectrumGreen or SpectrumRed as described (22).

Confocal microscopy. Images were captured with a Zeiss (Thornwood, NY) LSM 510 NLO laser scanning confocal microscope using a Zeiss $63\times$ Apochromat oil immersion lens (numerical aperture, 1.4; working distance, 0.09 mm) with Z-step sizes of 1.0 to $0.5 \mu\text{m}$ and $1,024 \times 1,024$ resolution ($\sim 0.05 \mu\text{m}$ pixels).

Results

A female patient originally diagnosed and treated for an ER-positive primary breast cancer underwent thoracentesis after presenting 8 years later with a pleural effusion. An aliquot of the pleural fluid was removed for clinical assays at which time the tumor cells were reported to be ER-negative, but with some PR positivity. The remaining tumor cells were precipitated and

Figure 1. Breast cancer cells from a pleural effusion, their growth as a mouse tumor, and isolation of an immortalized stromal cell line (BJZ3) derived from the xenograft. *A*, BC6 pleural effusion cells (adherent or floating cells) were separately xenografted into each fourth mammary gland and grown into tumors for 12 weeks. Both cell types yielded similar tumors. *B*, one tumor was excised and stained with H&E. Histopathologic examination shows a poorly differentiated adenocarcinoma with signet ring features (*arrow*) in a desmoplastic stromal background (***); magnification, $\times 200$. *C*, mouse and human cells were stained for mouse Cot-1 (*red*) or human Cot-1 (*green*); magnification, $\times 200$. *D*, immunohistochemistry for ER with the monoclonal antibody 1D5. Cells in the remaining tumor segment were dispersed, cultured, and a permanent cell line, BJZ3, was established. *E*, BJZ3 cells at passage 15; magnification, $\times 40$. BJZ3 cells were stained with (*F*) anti- α -smooth muscle actin (*SMA*) or (*G*) anti-cytokeratin 7 (*CK7*). HeLa human cervical carcinoma cells served as controls. Nuclei were counterstained with DAPI.



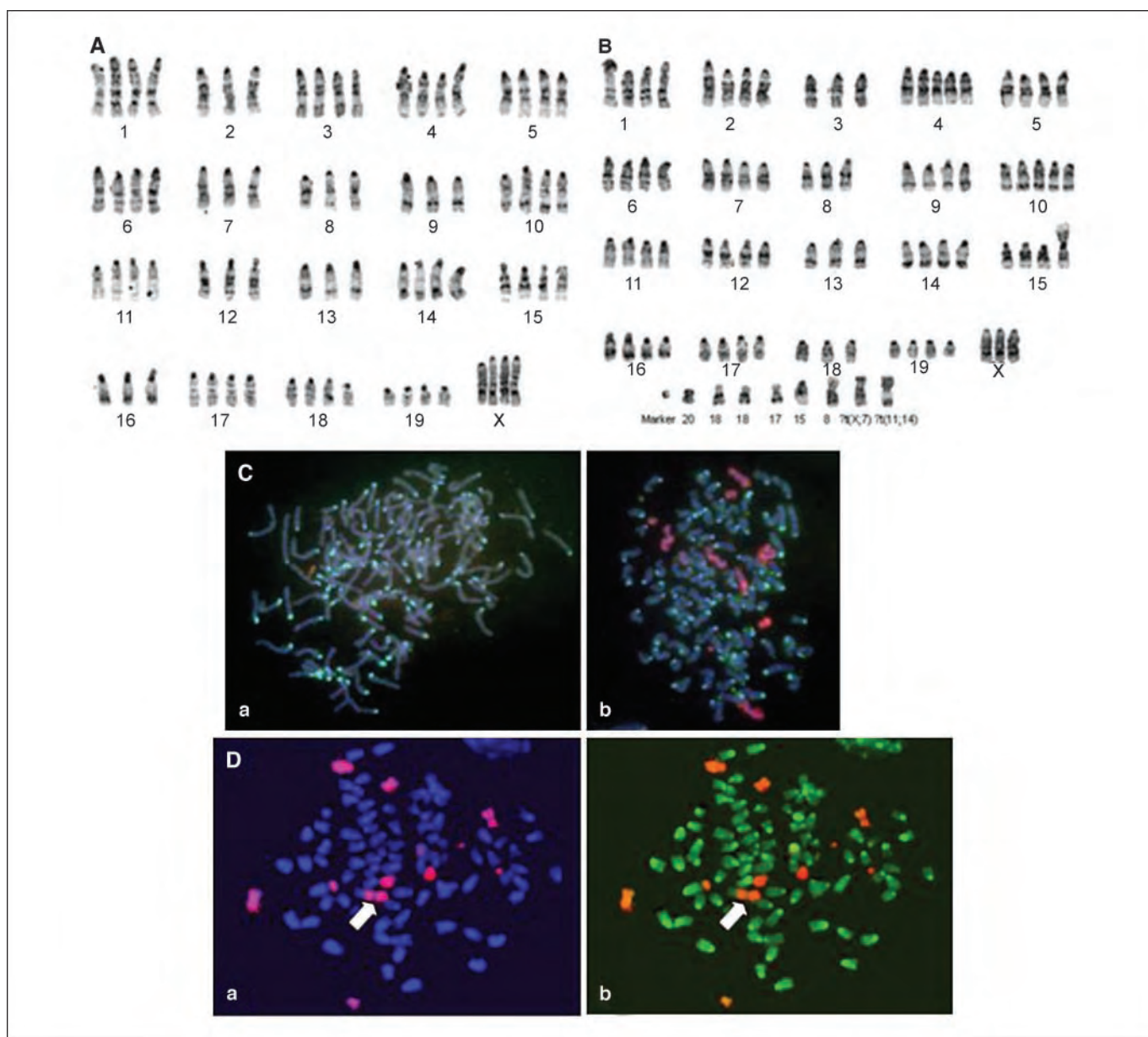


Figure 2. Karyotype analysis of BJ3Z cells shows hybrid cells that contain both mouse and human chromosomes. *A*, karyotype of one polyploid BJ3Z cell showing only mouse chromosomes. *B*, karyotype of one BJ3Z cell containing both mouse and human chromosomes (*bottom row*). Human chromosomes shown from left to right are: Marker, Chromosome 20, 18, 18, 17, 15, 8 ?t(x;7), ?t(11;14). *C*, metaphase spreads from BJ3Z cells hybridized with mouse Cot-1 DNA labeled with SpectrumGreen, and human Cot-1 DNA labeled with SpectrumRed showing: (*a*) a cell containing only mouse (*green*) chromosomes and (*b*) a cell containing both mouse (*green*) and human (*red*) chromosomes. Chromosomes are counterstained blue with DAPI. *D*, dual-color FISH of a metaphase spread using SpectrumRed-labeled human Cot-1/SpectrumGreen-labeled mouse Cot-1 and counterstained with DAPI showing: (*a*) blue/red channels or (*b*) green/red channels. *Arrows*, translocated chromosome.

incubated *in vitro* for 72 hours in the presence of penicillin/streptomycin to remove debris. Four million adherent or floating cells from the effusion (named BC6 cells), in 100% Matrigel, were then implanted into the mammary glands of 6-week-old, ovariectomized *nu/nu* mice, and supplemented with a 17 β -estradiol releasing pellet (23) in view of the possible hormone dependence of the patient's disease.

Solid tumor xenografts (Fig. 1A) of variable size were removed 12 weeks later, sectioned for histopathologic examination and immunohistochemical studies, and/or suspended and cultured *in vitro*. Histology of a representative tumor (Fig. 1B) shows a

poorly differentiated adenocarcinoma (arrow), morphologically consistent with the original diagnosis of a poorly differentiated infiltrating ductal carcinoma of the breast, in a desmoplastic stromal background (asterisk). The tumors contained both mouse and human cells as shown by Cot-1 staining for mouse (*red*) or human (*green*) DNA (Fig. 1C). Many cells were ER positive (Fig. 1D), suggesting that the receptors were reexpressed in the estrogenized solid tumor microenvironment.

Several cell lines were obtained from the solid tumors, one of which, BJ3Z, is shown in Fig. 1E. Their characteristic spindle-shaped fibroblastic morphology suggests that the cells are of

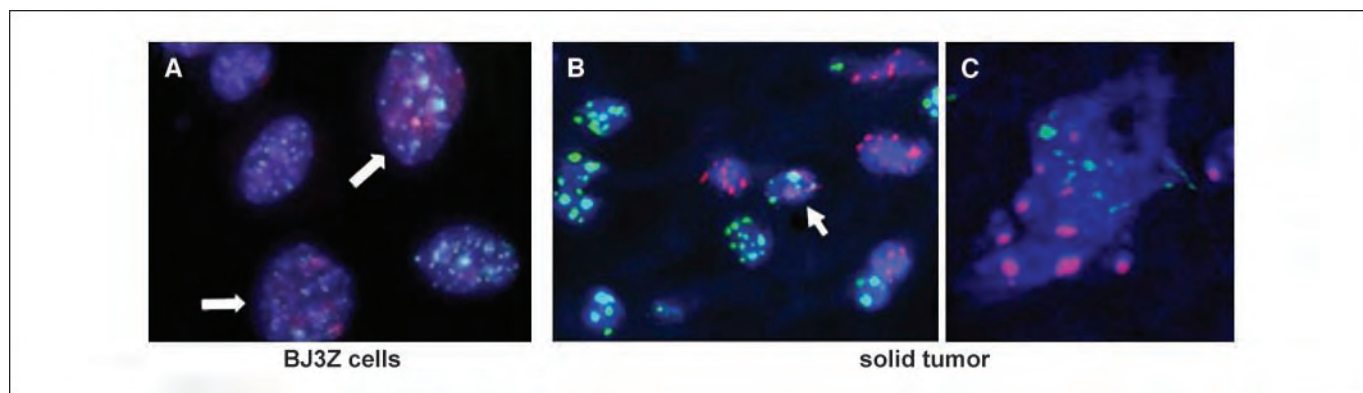


Figure 3. Hybrid mouse/human interphase nuclei are present in cells and solid tumors. *A*, interphase nuclei from BJ3Z hybridized with mouse DNA labeled with Cot-1 SpectrumGreen and human Cot-1 DNA labeled with SpectrumRed. *Arrows*, hybrid cells. *B*, interphase nuclei from a solid tumor xenograft like the one shown in Fig. 1*A* (*arrow*, hybrid cell). *C*, confocal microscopy of dual-color FISH-labeled solid tumor xenograft showing a hybrid nucleus. A representative Z stack image using a red and green filter. Z-stack images were exported as a movie that can be viewed as Supplementary Material (Movie S1).

stromal origin; probably mouse. This assignment was confirmed by presence of α -smooth muscle actin, a marker of myofibroblasts associated with reactive stroma (Fig. 1*F*), and by the absence of human cytokeratin 7 (Fig. 1*G*). In addition, BJ3Z cells were positive for stromal cell-derived factor 1 and vimentin (data not shown), further indices of activated stroma.

Because the mouse stroma supporting growth of the human tumor xenograft *in vivo* was presumed to be normal at the outset, immortalization of mouse BJ3Z cells in culture after a period of crisis is evidence that they had become transformed. Indeed,

analysis of 100 metaphase spreads and 13 karyotypes confirmed the mouse assignment, and showed that 70% of cells were polyploid, averaging 72 to 83 ($\sim 4n$) chromosomes (Fig. 2*A*). However, distinct human chromosomes were detected among the mouse chromosomes in $\sim 30\%$ of spreads and karyotype analyses of these cells revealed distinct human banding patterns (Fig. 2*B*, *bottom row*). Dual-color fluorescence *in situ* hybridization (FISH) of 42 metaphases showed 26 cells (62%) with all green (mouse) painted chromosomes (Fig. 2*C*, *a*) and 16 (38%) with a combination of red (human) and green (mouse) chromosomes (Fig. 2*C*, *b*). These

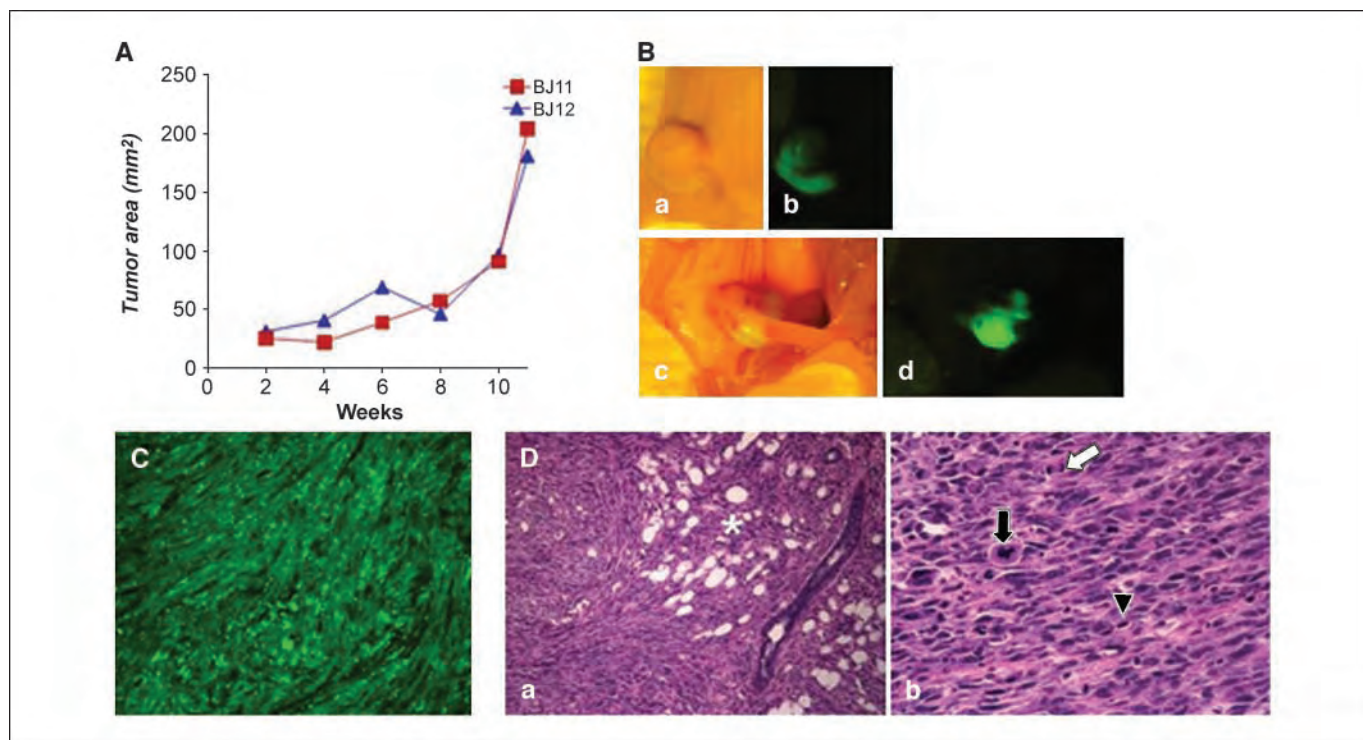


Figure 4. BJ3Z stromal cells are tumorigenic. BJ3Zg cells were injected bilaterally into the fourth mammary gland of ovariectomized nude mice and grown into tumors for 11 weeks. *A*, total tumor burden per mouse, in two mice (BJ11 and BJ12). *B*, (*top*) fluorescent whole body imaging using: (*a*) white light and (*b*) a 470 nm excitation filter and 515 nm viewing filter; (*bottom*) fluorescent intravital imaging under: (*c*) white light or (*d*) above filters. *C*, fluorescence imaging of BJ12 histologic sections; magnification, $\times 200$. *D*, H&E-stained section of BJ12 tumor showing: (*a*) a spindle cell tumor aggressively infiltrating normal mammary adipose tissue and entrapping a mammary duct (*); magnification, $\times 100$; (*b*) exhibiting cytologic pleomorphism, brisk mitotic rate (*white arrow*, mitotic figure), atypical (multipolar) mitoses (*black arrow*) and single cell necrosis (*black arrowhead*); magnification, $\times 400$.

16 synkaryons averaged 75 to 89 chromosomes which included the recurrent presence of human chromosomes 3, 5, 8, der(?)t(11;14), 15, 17, 18, 19, 20, 21, der(X)t(X;7) among the polyploid mouse complement. A few of these (8%) were found to have mouse/human translocations (Fig. 2D a, b, arrows). Two-hundred consecutive interphase BJ3Z nuclei (Fig. 3A) showed an even higher proportion (64%) of synkaryons than did the mitotic cells, suggesting a decrement in cell division rate among the hybrid cells. Indeed, karyotype analysis of later passage cells shows genetic drift, a decrease in the average number of chromosomes (72-83 versus 60-73 in early versus late passage, respectively), and gradual deletion of the human chromosomes (data not shown).

To determine whether the mouse stroma/human epithelial cell fusions occurred *in vitro* or were present in the solid tumor xenografts prior to culture, tumors taken directly from mice were paraffin embedded, sectioned, and probed with red (human) or green (mouse) fluorescent Cot-1. Figure 3B shows interphase nuclei in solid tumors that express only mouse (*green*), only human (*red*), or hybrid mouse/human chromatin (*arrow*). The fluorors were then reversed so that human Cot-1 was tagged green, and mouse Cot-1 was tagged red, and solid tumor sections were reprobbed and analyzed by laser scanning confocal microscopy (Fig. 3C). A representative Z-stack image shows blue DNA including red and green chromosomes, confirming the existence of hybrid cells in the solid tumor. A movie showing a three-dimensional view of a cell containing both mouse and human DNA is available online at the journal's web site for viewing as Supplementary Material (Movie S1).

To determine whether the mouse mammary stromal cell line was tumorigenic, BJ3Z cells were fluorescently tagged by transduction with retroviruses expressing ZsGreen. Bright green cells were isolated by flow cytometry, and 1 million cells were injected bilaterally into the fourth mammary gland of ovariectomized nude mice. Tumors grew slowly initially, then underwent accelerated, exponential growth. Figure 4A shows the growth pattern and average bilateral tumor area in two different mice. Figure 4B (a and b) shows a tumor that fluoresces green in a mouse, and Fig. 4B (c and d) shows a small, green fluorescent tumor in the fourth mammary gland detected after necropsy and dissection. These data confirm that the tumors developed from the injected exogenous stromal cells and not from endogenous normal mouse stroma. Histology and fluorescence microscopy confirm the BJ3Z origin of the tumors (Fig. 4C). Histopathologic examination shows a biologically aggressive spindle cell tumor with features of high-grade malignancy, including aggressive infiltration of mammary tissue (Fig. 4D, a) and cytologic pleomorphism with brisk mitotic rate, atypical multipolar mitoses, and single cell necrosis (Fig. 4D, b). The histopathologic features of the tumors indicate that these new stromal-derived cells are highly aggressive.

Discussion

Inherent in malignant progression is the acquisition of cell subpopulations exhibiting cytogenetic abnormalities characterized by aneuploidy and chromosomal rearrangements. Multiple mechanisms can give rise to aneuploid cells and genomic instability, including mutation of key genes, or cell cycling defects with associated inactivation of tetraploid checkpoints (24). Because spontaneous fusion between cells of the same species *in vivo* is almost impossible to detect, little is known about this process. Exceptions involve cell fusion as part of normal development including fusion of egg and sperm, formation of muscle cell

syncytia, or the syncytiotrophoblast of pregnancy (24, 25). However, spontaneous cell fusion between phenotypically distinct cells may represent an understudied mechanism for the generation of aneuploidy and diversity among cancer cells. There are rare reports of *in vivo* tumor cell fusion. One study published >30 years ago described the formation of highly aggressive tumors arising from human/hamster cell hybrids (26). Another, using chimeric mice, reported the formation of tumors that contained markers of both parental strains (27). The mechanisms for such "illicit" cell fusion (28) *in vivo* are unknown. *In vitro*, such fusion can be caused by a variety of agents including viruses (28), fusogenic proteins, and chemicals like polyethylene glycol (18).

The presence of hybrid cells in the solid tumors we describe here is evidence of a spontaneous fusogenic event between the normal stroma of the mouse mammary gland and the malignant human tumor cells embedded within them. In this regard, we observe rapid (<10 days) colonization by blood vessels and stroma of the Matrigel-encased tumor cells in mice (data not shown). Although we cannot definitively comment on the frequency of such fusogenic events, the fact that it was detected the first time the primary human tumor cells were implanted into mice suggests that the phenomenon may be quite common. Because the primary tumor cells were derived from a metastatic pleural effusion, their aggressiveness was already established. We speculate therefore, that similar fusogenic events may be especially prevalent at metastatic sites, in which case, they would involve the normal stroma of the distant host organ and the malignant epithelial cells that arrive there.

Our data prompt us to hypothesize that through fusogenic events, malignant epithelial cells can acquire the ability to genetically transform their stromal microenvironment. Previous studies have shown that activated stroma is involved in tumorigenesis, and that within malignant lesions, it supports angiogenesis and extracellular matrix remodeling (29, 30). We propose that in established tumors, activated stroma may also be genetically transformed, enhancing aggressiveness and metastatic potential because it is composed of hybrid cell variants expressing properties that differ from those of either parental cell (18, 31, 32). That is, when genetic alterations are induced in stroma by its malignant epithelial partner, the resultant tumor—now a mixture of transformed cell types—will augur a poor prognosis for the patient. Indeed it is possible that highly aggressive metaplastic breast cancers, exhibiting mixed epithelial/mesenchymal origins of unknown etiology, arise by such a mechanism.

In sum, cell fusion can be an engine of genetic variability that even within a tumor generates cells with new, possibly more aggressive properties; a hallmark of cancer progression. Such a mechanism could also explain the outgrowth of drug-resistant cell subpopulations and suggests that even for adenocarcinomas, therapies might need to target stromal cells. This is the first demonstration, to our knowledge, of genetic transformation of stroma by malignant epithelium in a solid tumor.

Acknowledgments

Received 4/21/2006; revised 6/9/2006; accepted 6/20/2006.

Grant support: NIH (CA 26869), the National Foundation for Cancer Research, the Breast Cancer Research Foundation, and the Avon Foundation. Support was also provided by the University of Colorado Health Sciences Center's Light Microscopy Core, and the University of Colorado Cancer Center's Cytogenetics and Flow Cytometry Cores.

The costs of publication of this article were defrayed in part by the payment of page charges. This article must therefore be hereby marked *advertisement* in accordance with 18 U.S.C. Section 1734 solely to indicate this fact.

Special thanks to Robert W. Burke and Steven Fadul for advice and assistance.

References

1. Schor SL, Schor AM. Phenotypic and genetic alterations in mammary stroma: implications for tumour progression. *Breast Cancer Res* 2001;3:373–9. Epub 2001 Sep 6.
2. Walker RA. The complexities of breast cancer desmoplasia. *Breast Cancer Res* 2001;3:143–5. Epub 2001 Feb 1.
3. Cukierman E. A visual-quantitative analysis of fibroblastic stromagenesis in breast cancer progression. *J Mammary Gland Biol Neoplasia* 2004;9:311–24.
4. Liotta LA, Kohn EC. Stromal therapy: the next step in ovarian cancer treatment. *J Natl Cancer Inst* 2002;94:1113–4.
5. Dvorak HF. Tumors: wounds that do not heal. Similarities between tumor stroma generation and wound healing. *N Engl J Med* 1986;315:1650–9.
6. Orimo A, Gupta PB, Sgroi DC, et al. Stromal fibroblasts present in invasive human breast carcinomas promote tumor growth and angiogenesis through elevated SDF-1/CXCL12 secretion. *Cell* 2005;121:335–48.
7. Hanahan D, Weinberg RA. The hallmarks of cancer. *Cell* 2000;100:57–70.
8. Cullen KJ, Smith HS, Hill S, Rosen N, Lippman ME. Growth factor messenger RNA expression by human breast fibroblasts from benign and malignant lesions. *Cancer Res* 1991;51:4978–85.
9. Basset P, Wolf C, Chambon P. Expression of the stromelysin-3 gene in fibroblastic cells of invasive carcinomas of the breast and other human tissues: a review. *Breast Cancer Res Treat* 1993;24:185–93.
10. Dano K, Romer J, Nielsen BS, et al. Cancer invasion and tissue remodeling—cooperation of protease systems and cell types. *APMIS* 1999;107:120–7.
11. Jessani N, Humphrey M, McDonald WH, et al. Carcinoma and stromal enzyme activity profiles associated with breast tumor growth *in vivo*. *Proc Natl Acad Sci U S A* 2004;101:13756–61. Epub 2004 Sep 8.
12. Hu M, Yao J, Cai L, et al. Distinct epigenetic changes in the stromal cells of breast cancers. *Nat Genet* 2005;37:899–905. Epub 2005 Jul 10.
13. Paterson RF, Ulbright TM, MacLennan GT, et al. Molecular genetic alterations in the laser-capture-microdissected stroma adjacent to bladder carcinoma. *Cancer* 2003;98:1830–6.
14. Wernert N, Locherbach C, Wellmann A, Behrens P, Hugel A. Presence of genetic alterations in microdissected stroma of human colon and breast cancers. *Anticancer Res* 2001;21:2259–64.
15. Moinfar F, Man YG, Arnould L, Bratthauer GL, Ratschek M, Tavassoli FA. Concurrent and independent genetic alterations in the stromal and epithelial cells of mammary carcinoma: implications for tumorigenesis. *Cancer Res* 2000;60:2562–6.
16. Hida K, Hida Y, Amin DN, et al. Tumor-associated endothelial cells with cytogenetic abnormalities. *Cancer Res* 2004;64:8249–55.
17. Rosen PP. *Rosen's breast pathology*. 2nd ed. Philadelphia (PA): Lippincott Williams & Wilkins; 2001.
18. Duelli D, Lazebnik Y. Cell fusion: a hidden enemy? *Cancer Cell* 2003;3:445–8.
19. Sartorius CA, Harvell DM, Shen T, Horwitz KB. Progesterone initiates a luminal to myoepithelial switch in estrogen-dependent human breast tumors without altering growth. *Cancer Res* 2005;65:9779–88.
20. Jacobsen BM, Richer JK, Schittone SA, Horwitz KB. New human breast cancer cells to study progesterone receptor isoform ratio effects and ligand-independent gene regulation. *J Biol Chem* 2002;277:27793–800.
21. Lee JJ, Warburton D, Robertson EJ. Cytogenetic methods for the mouse: preparation of chromosomes, karyotyping, and *in situ* hybridization. *Anal Biochem* 1990;189:1–17.
22. Li FX, Zhu JW, Tessem JS, et al. The development of diabetes in E2f1/E2f2 mutant mice reveals important roles for bone marrow-derived cells in preventing islet cell loss. *Proc Natl Acad Sci U S A* 2003;100:12935–40. Epub 2003 Oct 17.
23. Sartorius CA, Shen T, Horwitz KB. Progesterone receptors A and B differentially affect the growth of estrogen-dependent human breast tumor xenografts. *Breast Cancer Res Treat* 2003;79:287–99.
24. Storchova Z, Pellman D. From polyploidy to aneuploidy, genome instability and cancer. *Nat Rev Mol Cell Biol* 2004;5:45–54.
25. Taylor MV. Muscle differentiation: how two cells become one. *Curr Biol* 2002;12:R224–8.
26. Goldenberg DM, Pavia RA, Tsao MC. *In vivo* hybridisation of human tumour and normal hamster cells. *Nature* 1974;250:649–51.
27. Fortuna MB, Dewey MJ, Furmanski P. Enhanced lung colonization and tumorigenicity of fused cells isolated from primary MCA tumors. *Cancer Lett* 1990;55:109–14.
28. Duelli DM, Hearn S, Myers MP, Lazebnik Y. A primate virus generates transformed human cells by fusion. *J Cell Biol* 2005;171:493–503.
29. Tlsty TD, Hein PW. Know thy neighbor: stromal cells can contribute oncogenic signals. *Curr Opin Genet Dev* 2001;11:54–9.
30. Sternlicht MD, Lochter A, Sympon CJ, et al. The stromal proteinase MMP3/stromelysin-1 promotes mammary carcinogenesis. *Cell* 1999;98:137–46.
31. Barski G, Sorieul S, Cornefert F. "Hybrid" type cells in combined cultures of two different mammalian cell strains. *J Natl Cancer Inst* 1961;26:1269–91.
32. Larizza L, Schirmacher V. Somatic cell fusion as a source of genetic rearrangement leading to metastatic variants. *Cancer Metastasis Rev* 1984;3:193–222.



Original article

Thyroid Outcome During Long-Term Gonadotropin-Releasing Hormone Agonist Treatments for Idiopathic Precocious Puberty

Francesco Massart^{a,*}, Joshua Chuck Harrell^b, Giovanni Federico^a, and Giuseppe Saggese^a

^a*Pediatric Endocrine Center/Department of Pediatrics, University of Pisa, Pisa, Italy*

^b*University of Colorado Health Sciences Center, Aurora, Colorado*

Manuscript received July 19, 2006; manuscript accepted September 29, 2006

Abstract

Purpose: To examine the effects of long-term gonadotropin-releasing hormone agonist (GnRHa) administration on thyroid function in children affected by central precocious puberty (CPP).

Methods: We retrospectively evaluated circulating thyroid hormones in 73 GnRHa-treated girls who were diagnosed with idiopathic CPP. Monthly depot injections (.1 mg/body kg) of leuprorelin acetate (LA) and of triptorelin (TR) were continuously administered for $40.4 \pm .7$ months to 34 and 39 CPP patients, respectively. Serum levels of thyrotropin (TSH), free triiodothyronine (FT3), free thyroxine (FT4), and thyroid antibodies were determined at baseline and after 6, 12, 18, 24, 30, 36, and 40 months of GnRHa administration.

Results: While there was no difference in FT4 release ($p > .05$), FT3 levels significantly declined during both LA and TR treatments from untreated baseline ($p < .05$). Opposite to circulating FT4 and FT3 values ($p > .05$), FT3/FT4 ratio was significantly different among LA and TR groups ($p < .05$). Both GnRHa treatments did not affect TSH secretion ($p > .05$); however, LA induced lower TSH values than TR ($p < .05$).

Conclusions: There is no evidence of thyroid dysfunction during both GnRHa treatments, though changes in TSH, FT3, and FT3/FT4 ratios were noted. Finally, monitoring of thyroid activity during GnRHa administration is not required. © 2007 Society for Adolescent Medicine. All rights reserved.

Keywords:

Gonadotropin-releasing hormone agonist; Leuprorelin acetate; Precocious puberty; Thyroid; Triptorelin

Since the 1980s, long-acting gonadotropin-releasing hormone agonist (GnRHa) preparations have been the most effective treatment for children affected by idiopathic central precocious puberty (CPP) [1–3]. Administration of GnRHa drugs, such as leuprorelin acetate (LA) and triptorelin (TR), results in an initial increase in serum luteinizing hormone (LH) and follicle-stimulating hormone (FSH) levels and a corresponding rise in circulating estrogens and androgens [1,2,4]. Prolonged administration of these drugs inhibits gonadotropin secretion by downregulating GnRH receptors, therapeutically inducing a hypogonadic state [1–3].

Many GnRHa formulations are available today, and usually differ from the native GnRH decapeptide by some amino acid substitutions. For example, TR differs from native GnRH by one D -tryptophan at the sixth position (Trp⁶), whereas LA substitutes amino acids at the sixth (Leu⁶) and tenth (N-ethylamide¹⁰) positions [4]. The amino acid substitutions increase the drug's resistance to metabolism, prolong its action, and increase its potency. Although TR and LA are different biochemically, they are clinically regarded as identical and are usually given intramuscularly (IM) at 4-week intervals to pediatric patients [5–8].

Because the amino acid sequences of the depot GnRHa are different, it is possible that the clinical potency and the duration of drug action are not the same [6]. Few clinical studies directly comparing different GnRHa preparations have been performed in CPP children [9,10]. In addition, most adverse effects or specific mechanisms by which

*Address correspondence to: Francesco Massart, M.D., Ph.D., Pediatric Endocrine Center/Department of Pediatrics, University of Pisa, Via Roma 67, 56125 Pisa, Italy.

E-mail address: massart@med.unipi.it

GnRHa affects hormonal secretion other than gonadotropins are still unknown [11]. We recently reported asymptomatic hyperprolactinaemia as a side effect of TR treatment [12].

Next to general concerns about GnRHa treatment safety, reports on the relationship between GnRHa and thyroid function are controversial. Some authors indicate that GnRHa themselves have no effect on the serum levels of thyroid hormones or pituitary thyrotropin (TSH) [13,14], whereas others report that GnRHa may induce autoimmune thyroid dysfunction [15–20]. To date, sporadic data are available for children concerning GnRHa-induced thyroid status [19].

As result of a hepatic first-pass effect, the oral administration of estrogens causes a dose-dependent increase in the serum levels of thyroxine-binding globulin (TBG) as well as other hormone-binding proteins synthesized in the liver [21,22]. This phenomenon is similar to the effects of pregnancy when circulating estrogen levels increase by more than two orders of magnitude by the third trimester [22]. The elevation of TBG levels raises the bound fraction of thyroxine, and lowers its free fraction. Also, total thyroxine and, to a lesser extent, total triiodothyronine increase in any hyperestrogenemic state, including oral contraceptive use and pregnancy [22]. In this view, following GnRHa-induced hypogonadism after premature awakening of hypothalamic-pituitary-ovary axis might dysregulate child thyroid function.

The present study was undertaken to chart thyroid function during long-term GnRHa administration. We compared circulating levels of TSH, free triiodothyronine (FT3), free thyroxine (FT4), antibodies to thyroglobulin (TGAb), and antibodies to thyroperoxidase (TPOAb) in 73 CPP girls treated with TR and LA drugs. We found that long-term treatment with TR or LA did not induce thyroid dysfunction in euthyroid children, although both these GnRHa slightly inhibited thyroid secretion by different mechanisms.

Methods

Patient population

To assess thyroid function during long-term GnRHa treatment, we retrospectively analyzed clinical data of CPP girls attended as outpatients at the Pediatric Endocrine Center of Pisa between 1998 and 2004. After local Institutional Review Board approval, informed consent was obtained for all parents of patients prior to the study. The inclusion criteria in the study were: (1) being a female affected by idiopathic CPP; (2) being continuously GnRHa-treated for more than 37 months; (3) one IM monthly-depot GnRHa formulation used during the treatment; and (4) GnRHa treatment withdrawal at bone age of 12–12.5 years. Furthermore, we excluded from this analysis patients with GnRHa-induced hyperprolactinaemia [12].

Seventy-three Caucasian girls affected by idiopathic CPP were found to fit the above study criteria. They were GnRHa-treated for 37.2–43.3 months (mean = $40.4 \pm .7$ months) with LA and TR drug formulations. At CPP diagnosis, all patients had a history of increased growth velocity, Tanner breast stage of at least 2, and bone age was advanced more than 1 year; LH and FSH responses to the GnRH stimulation test (100 mg/m^2 , intravenous [IV] bolus dose) were in the pubertal range [23]. Clinical CPP diagnosis was also confirmed by $17\text{-}\beta$ -estradiol (E_2) levels $\geq 25 \text{ pg/mL}$ and by age ≤ 8 years. No patient had any evidence of: (1) progressive organic central nervous system disorders by computer tomography or magnetic resonance imaging, (2) identifiable adrenal or gonadal pathology, (3) thyroid or growth hormone deficiency, (4) or any other central or peripheral causes of precocious puberty.

Thirty-four (46.6%) girls were treated with leuprorelin acetate IM (Takeda Chemical Industries Ltd, Osaka, Japan) at a mean dose of .1 mg/body kg every 28 days (LA group), whereas 39 (53.4%) received triptorelin depot IM (Decapeptyl, Ipsen Pharma Biotech S.A., Toulon Cedex, France) at a mean dose of .1 mg/body kg every 28 days (TR group). CPP patients were randomly assigned to LA or TR treatment. The GnRHa doses were adjusted during the treatment according to patient weight.

GnRHa suppression of gonadotropin secretion was checked every 6 months by radioimmunoassays (RIA) for serum levels of LH, FSH, and E_2 in both LA and TR groups.

Hormone assays

Serum levels of TSH, FT3, FT4, TGAb, and TPOAb were assayed before (untreated baseline) and during GnRHa treatment at 6-month intervals (at 6, 12, 18, 24, 30, 36, and 40 months). TSH, FT3, FT4, TGAb, and TPOAb were measured using commercial RIA kits (TSH, FT3, FT4, Techno Genetics, Milan, Italy; TGAb, Biocode-Hycle, Liege, Belgium; TPOAb, Brahms, Hennigsdorf, Germany). In our hands, these RIA assays had within-assay coefficients of variation of 6.8%, 5.5%, 5.1%, 5.8%, and 5.5%, while between-assay variability was 4%, 6.8%, 7.5%, 8.4%, and 7.6% for TSH, FT3, FT4, TGAb, and TPOAb, respectively. The detection limit of RIA method was $.01 \mu\text{U/mL}$ for TSH, $.5 \text{ pg/mL}$ for FT3, $.8 \text{ pg/mL}$ for FT4, 3 IU/mL for TGAb, and 3 IU/mL for TPOAb. Normal ranges of TSH, FT3, FT4, TGAb, and TPOAb were $.3\text{--}3.6 \mu\text{U/mL}$, $2.3\text{--}5.6 \text{ pg/mL}$, $5.6\text{--}13.0 \text{ pg/mL}$, $0\text{--}50 \text{ IU/mL}$, and $0\text{--}10 \text{ IU/mL}$ respectively. All blood samples from each subject were analyzed in single assay.

Statistical analysis

Data were expressed as mean \pm standard deviation (SD) unless otherwise stated. Statistical evaluation was performed using one-way analysis of variance (ANOVA) and Pearson's correlation (r) where multiple samples were ob-

Table 1
Clinical data of CPP patients at the start of GnRha administration

	TR group (n = 39)	LA group (n = 34)
Chronological age (yr)	7.4 ± .9	7.2 ± 1.2
Pubertal stage: median (range)		
Tanner breast	2 (2-3)	2 (2-3)
Tanner pubic hair	2 (2-3)	2 (2-3)
Basal LH (IU/L)	2.8 ± 1.5	2.4 ± .9
Basal FSH (IU/L)	3.6 ± .9	4.0 ± 1.3
E ₂ (pg/mL)	27.9 ± 2.0	28.4 ± 1.7
Therapy months	4.2 ± .6	4.5 ± .4

Note: ^a *p* < .05 TR vs. LA group.

tained. When two sets of data were compared (e.g., LA vs. TR series), a paired and an unpaired Student's t-test was employed. A two-tailed significance test was used for all comparisons and *p* < .05 was considered statistically significant. Bonferroni's adjustment to the *p*-value was applied where appropriate.

Results

At the start of GnRHa treatment, the auxological characteristics of CPP subjects treated with TR and LA were statistically similar (*p* > .05; Table 1). During GnRHa treatment, down-regulation of the pituitary-gonadal axis was confirmed by suppressed LH, FSH, and E₂ levels. They fell significantly during TR treatment with serum values of .76 ± .5 IU/L, 1.23 ± .6 IU/L, and 13.6 ± 1.5 pg/mL, respectively (*p* < .001 for all three hormones as compared with their levels before TR treatment). During LA administration, circulating levels of LH, FSH, and E₂ were .8 ± .5 IU/L, 1.5 ± .6 IU/L, and 14.3 ± 1.3 pg/mL, respectively (*p* < .001 for all three hormones as compared with their levels before LA treatment). Regarding LH, FSH, and E₂, no significant difference was found among LA and TR groups before and during GnRHa treatment (*p* > .05).

The effect of GnRHa administration (LA plus TR groups) on thyroid function was evaluated by comparing circulating TSH, FT4, and FT3 values at diagnosis (baseline) and throughout 40 months of GnRHa treatment (Table 2). While TSH secretion was not affected by GnRHa administration (*p* > .05 for any levels vs. pretherapy), FT4 levels slightly declined from 9.3 ± 1.7 pg/mL (untreated

Table 2
Thyroid function during GnRHa treatment

<GnRHa (months)	0	6	12	18	24	30	36	40
TSH (μU/mL)	2.1 (.9)	2.4 (1.2)	2.2 (1.0)	2.5 (.9)	2.1 (1.0)	2.0 (.7)	2.3 (.7)	2.1 (.9)
FT4 (pg/mL)	9.3 (1.7)	9.4 (1.7)	9.4 (1.8)	9.2 (1.6)	8.8 (.9)	8.7 (1.6)	8.8 (2.2)	8.2 (1.9)
FT3 (pg/mL)	4.3 (.5)	4.2 (.6)	4.1 (.5) ^a	4.0 (.7) ^a	3.7 (.7) ^a	3.7 (.5) ^a	3.8 (.7) ^a	3.5 (.6) ^a
FT3/FT4 ratio	.463 (.013)	.446 (.005) ^a	.434 (.004) ^a	.438 (.007) ^a	.426 (.004) ^a	.429 (.003) ^a	.431 (.01) ^a	.424 (.002) ^a

Mean (SD); ^a *p* < .05 vs. untreated baseline.

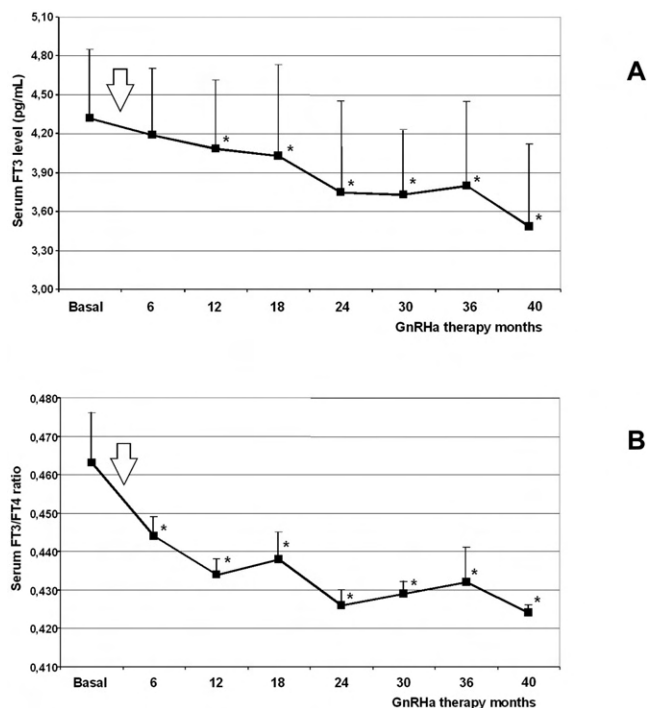


Figure 1. (A) Serum FT3 level (± SD) in CPP children during 40 months of GnRHa. (B) Mean FT3/FT4 ratio (± SD) in GnRHa-treated CPP children. Open arrow indicates GnRHa treatment start (**p* < .05 vs. untreated baseline).

baseline) to 8.2 ± 1.9 pg/mL at 40 months of GnRHa therapy (*p* > .05 for any levels vs. pretherapy). These results were confirmed by ANOVA analysis (*p* > .05 for TSH and for FT4 data, respectively).

After 6 months of GnRHa treatment, mean FT3 levels showed a significant decline from a basal concentration of 4.3 ± .5 pg/mL to 3.5 ± .6 pg/mL at 40 months (*p* < .05 for six time points; Figure 1A). During GnRHa treatment, FT3 values positively correlated with FT4 (*r* = .983; *p* < .05), such as TSH secretion against serum levels of FT4 (*r* = .664; *p* < .05) and FT3 (*r* = .733; *p* < .05), respectively. Additionally, during GnRHa treatment, a declining trend in the FT3/FT4 ratio (*p* < .05 for all seven time points vs. basal level; Figure 1B) with significant correlation between the FT3/FT4 ratio and amount of TSH secreted (*r* = .814; *p* < .05) was detected. ANOVA analysis reported significant trends during GnRHa administration for FT3

Table 3
Comparison of TSH and thyroid hormone levels among LA- and TR-treated patients

	Months							
	0	6	12	18	24	30	36	40
TR group								
TSH ($\mu\text{U/mL}$)	2.0 (.9)	2.3 (1.2)	2.4 (1.1)	2.5 (1.0)	2.6 (1.2)	2.4 (.8)	2.5 (.6)	2.7 (1.1)
FT4 (pg/mL)	9.7 (1.7)	9.7 (1.8)	9.0 (1.6)	9.1 (1.6)	8.7 (.9)	8.5 (1.6)	8.8 (2.3)	8.2 (2.2)
FT3 (pg/mL)	4.3 (.6)	4.3 (.5)	4.1 (.6)	4.1 (.7)	4.0 (.5) ^a	3.8 (.3) ^a	3.9 (.6) ^a	3.7 (.5) ^a
FT3/FT4 ratio	.447 (.007)	.440 (.005)	.458 (.01)	.453 (.007)	.460 (.012)	.442 (.005)	.436 (.011)	.448 (.001)
LA group								
TSH ($\mu\text{U/mL}$)	2.3 (.9)	2.5 (1.3)	1.8 (.8) ^b	2.0 (.6) ^b	1.7 (.6) ^b	1.7 (.5) ^b	1.9 (.8) ^b	1.8 (.7) ^b
FT4 (pg/mL)	9.3 (1.9)	8.4 (.9) ^b	1.2 (2.0) ^b	9.3 (1.7)	9.5 (.5)	9.1 (1.6)	9.0 (1.0)	8.3 (.9)
FT3 (pg/mL)	4.3 (.4)	4.0 (.5)	3.9 (.5) ^a	3.8 (.7) ^a	3.4 (.8) ^a	3.7 (.7) ^a	3.8 (.8) ^a	3.4 (.7) ^a
FT3/FT4 ratio	.463 (.01)	.470 (.007) ^b	.382 (.005) ^{a,b}	.406 (.007) ^{a,b}	.354 (.006) ^{a,b}	.405 (.003) ^{a,b}	.397 (.01) ^{a,b}	.401 (.002) ^{a,b}

Mean (SD); ^a $p < .05$ vs. baseline for LA and TR group; ^b $p < .05$ TR vs. LA series.

($F = 2.423$; $p < .05$) and for the FT3/FT4 ratio ($F = 2.301$; $p < .05$), respectively.

Next, the LA and TR series were separately compared (Table 3). ANOVA analysis revealed that TSH levels were statistically different than baseline in the TR group ($F = 2.323$; $p < .05$) but not in the LA group ($F = 1.663$; $p > .05$). TSH levels were not different from basal levels in both GnRHa groups ($p > .05$, for all seven time points in both groups), however, LA-treated TSH values were significantly lowered compared to TR-treated TSH values from 12–40 months of GnRHa treatment ($p < .05$ for all six time points, LA vs. TR group; Figure 2A).

No difference in FT4 values were observed during 40-months of GnRHa administration in both LA and TR treatment groups ($p > .05$ for all seven time points vs. baseline). ANOVA analysis did not detect significant differences during GnRHa treatment ($p > .05$), and mean FT4 levels were not different between the TR and LA groups ($p > .05$, for TR vs. LA series). During GnRHa treatment, FT4 secretion was found to negatively correlate with TSH in both the LA ($r = -.423$; $p < .05$) and TR groups ($r = -.400$; $p < .05$).

Over time, both the LA and TR treatments reduced FT3 levels, although these values did not differ among the two groups ($p > .05$ LA vs. TR group) (Fig. 2B). FT3 was significantly lower than baseline after 12 months in the LA group ($p < .05$ for all six time points), and after 24 months in the TR group ($p < .05$ for all four time points). Furthermore, significant FT3 changes from untreated levels were assessed by ANOVA analysis for both TR ($F = 2.319$; $p < .05$) and LA treatment ($F = 2.501$; $p < .05$). During GnRHa treatment, FT3 secretion significantly correlated with TSH in the LA ($r = 0.595$; $p < .05$) but not in the TR group ($r = -.219$; $p > .05$), while a strong correlation was observed among FT3 and FT4 in the TR ($r = .925$; $p < .05$) but not in the LA group ($r = .199$; $p > .05$).

Regarding the FT3/FT4 ratio, ANOVA analysis detected a significant difference in the LA ($F = 2.537$; $p < .05$ vs. basal level) but not in the TR series ($p > .05$ vs. basal level). No difference was detected in TR-treated patients ($p > .05$

vs. pretherapy for all time points), whereas LA induced a significantly lower FT3/FT4 ratio than the basal level from 12–40 months of treatment ($p < .05$ for all six time points; Figure 2C). In addition, the FT3/FT4 ratio significantly correlated with TSH in the LA ($r = .843$; $p < .05$) but not in the TR group ($r = .330$; $p > .05$). TR-induced FT3/FT4 ratio was significantly higher than the LA series at 12, 18, 24, 30, 36, and 40 months ($p < .05$ LA vs. TR group).

The serum levels of thyroid antibodies, TGAb and TPOAb, were determined to not be present in all patients before and during GnRHa therapy ($p > .05$, vs. baseline; data not shown). Furthermore, no difference was detected among LA and TR group ($p > .05$, LA vs. TR series; data not shown). Also, none of TGAb and TPOAb levels were statistically different as assessed by ANOVA ($p > .05$).

Finally, GnRHa administration resulted in no difference in body mass index (BMI) among LA and TR treatment ($p > .05$; data not shown). None of the thyroid hormone levels were statistically associated with BMI before and during GnRHa treatment ($p > .05$; data not shown). No significant correlations were found between LH, FSH, or E_2 versus TSH, FT4, FT3, and FT3/FT4 ratio in both GnRHa groups ($p > .05$). Importantly, no treatment side effects were detected in both LA and TR groups.

Discussion

GnRHa drugs are used in the treatment of a wide variety of sex hormone-related diseases, including uterine leiomyoma, endometriosis, prostate, and breast cancer [1,2]. In the pediatric population, GnRHa drugs are mostly used to delay the effects of premature awakening of the hypothalamic-pituitary-gonadal axis in children with CPP [3,5,6].

In our Pediatric Endocrine Center, CPP patients are determined for GnRHa suppression of gonadotropin-ovary axis every 4–6 months by circulating LH, FSH, and E_2 levels. In these blood samples, thyroid status is also checked because we live in a moderate iodine-deficiency area [24]. Furthermore, hypothyroidism is in differential diagnosis

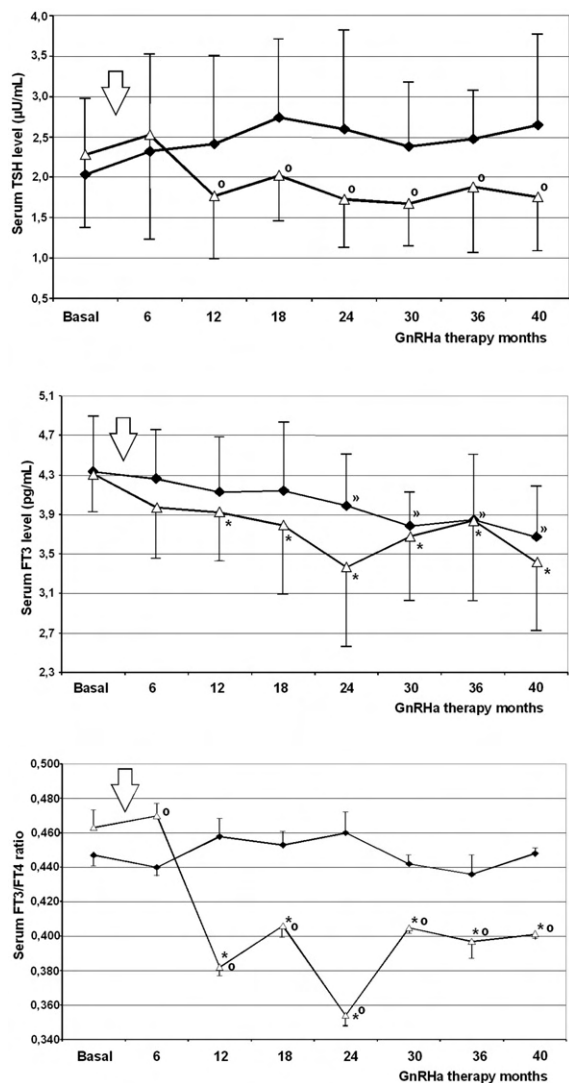


Figure 2. (A) Serum TSH release (\pm SD) in CPP children during 40 months of (LA) (open triangle) and TR treatment (full square). (B) FT3 values (\pm SD) in LA-treated (open triangle) and TR-treated (full square) CPP children. (C) Mean FT3/FT4 ratio (\pm SD) in CPP children during LA (open triangle) and TR treatment (full square). Open arrow indicates GnRHa treatment start (* and \geq $p < .05$ vs. baseline for LA and TR, respectively. ° $p < .05$ LA vs. TR series).

with precocious puberty and some authors reported GnRHa-induced thyroid dysfunction [15–20,25].

To our knowledge, there has been no data published on thyroid outcome in GnRHa-treated children. In this view, we compared two widely used GnRHa, TR and LA, that exhibit similar chemical structures, pharmacological profiles, and clinical outcomes [4,26]. Therefore, the present study was designed to test the clinical benefits of thyroid monitoring in children that were long-term GnRHa-treated.

Relatively few studies have investigated the effects of GnRHa treatment on the pituitary-thyroid axis. After 2–3 monthly depot injections of leuprolide acetate (D -Leu⁶,Des,Gly-NH₂¹⁰-Proethylamide⁹ GnRH; 3.75 mg), Chantilis et al [13] observed

GnRHa-treated women presented slight lower ($p > .05$) basal and TRH-induced TSH levels than untreated control women. Also, they did not detect any significant difference between FT3 and FT4 values [13]. These data are similar to those we observed in both GnRHa series during the first 6 months of therapy. Because we assayed significant differences compared to basal levels after 12–24 months of treatment, it is debatable whether thyroid dysfunction may result only from GnRHa administration longer than 12 months.

While no significant difference was detected in the FT4 levels during 40 months of treatment in both GnRHa series, there were quite different TSH and FT3 patterns among the LA and TR groups. After 6 months of therapy, LA significantly lowered FT3 values. Consistent with unaffected FT4, LA-induced TSH was slightly, but not significantly, decreased versus baseline. Indeed, the reduced FT3/FT4 ratio that occurred during treatment suggested LA may inhibit the conversion of T4 into T3, which mostly occurs at the extra-thyroid level. Interestingly, similar thyroid status was reported during amiodarone treatment [27].

On the other hand, TR seems to directly influence thyroid secretion. TR-induced FT3 release was statistically lower than pretherapy levels, whereas FT4 values presented a steady, though not significant, decline during TR administration. Both FT3 and FT4 declines were consistent with the constant FT3/FT4 ratio observed during TR treatment. In this view, the inhibitor effect of TR treatment on FT3 and FT4 release may be partially opposed by steady TSH increase. Finally, the clinical significance that TR treatment affects thyroid function was minimal.

To date, several reports suggest that painless autoimmune thyroiditis may develop during busserelin acetate, nafarelin, and leuprolide acetate treatment for uterine leiomyoma, endometriosis, or precocious puberty [15–20]. Most of these case reports were adult females without any background autoimmune thyroid diseases before GnRHa treatments (similar to our CPP patients). Moreover, the onset of thyroid dysfunction and GnRHa therapy are not coincidental in association because thyroid dysfunction developed at 3–4 months (range = 1–8 months) after initiation of GnRHa treatments [15–20]. In this regard, the latest development of autoimmune thyroiditis occurred in a 9-year-old CPP girl approximately 8 months after initiation of leuprolide acetate therapy [19]. To our knowledge, there has been no data published regarding TR or LA induction of autoimmune diseases. In the 73 CPP children tested in this study, normal values of TGAb and TPOAb were found during 40 months of GnRHa treatment. From our data and others [15–20], we hypothesize that the onset of risk is unlikely after the first 12 months of GnRHa treatment. However, our data excluded that chronic LA or TR treatments induce autoimmune thyroiditis.

Of special interest is that all CPP patients remained clinically euthyroid (serum TSH, FT3, FT4, and thyroid antibodies were found in the normal reference ranges) dur-

A

B

C

ing the study. Therefore, the major clinical issue raised by the data presented is that LA and TR did not induce thyroid dysfunction in euthyroid subjects, although both of these GnRHa slightly inhibit thyroid secretion, with different mechanisms. With substantial euthyroidism of GnRHa-treated subjects, we did not reveal any clinical usefulness to frequently check thyroid function during TR and LA administration. In our opinion, it may waste health resources and yield unnecessary discomfort for the patient.

Until now, there has been no consensus about the importance of monitoring thyroid function in GnRHa-treated children (unless clinical symptoms of thyroid dysfunction appear). We suggest obtaining TSH, FT4, FT3, and thyroid antibody levels before initiation of GnRHa therapy, and again at 8–12 months of such therapy. In cases of hormone impairment or antibody presence, thyroid function tests and ultrasound assessment are recommended to minimize the risk of undiagnosed thyroid dysfunction. Then, in our opinion, there is no need to routinely follow thyroid tests in GnRHa-treated patients unless clinical signs of thyroid disease development.

References

- [1] McArdle CA, Franklin J, Green L, et al. Signalling, cycling and desensitisation of gonadotrophin-releasing hormone receptors. *J Endocrinol* 2002;173:1–11.
- [2] Kiesel LA, Rody A, Greb RR, et al. Clinical use of GnRH analogues. *Clin Endocrinol* 2002;56:677–87.
- [3] Heger S, Sippell WG, Partsch CJ. Gonadotropin-releasing hormone analogue treatment for precocious puberty. Twenty years of experience. *Endocr Dev* 2005;8:94–125.
- [4] Lahlou N, Carel JC, Chaussain JL, et al. Pharmacokinetics and pharmacodynamics of GnRH agonists: Clinical implications in pediatrics. *J Pediatr Endocrinol Metab* 2000;13:723–37.
- [5] Bertelloni S, Baroncelli GI, Sorrentino MC, et al. Effect of central precocious puberty and gonadotropin-releasing hormone analogue treatment on peak bone mass and final height in females. *Eur J Pediatr* 1998;157:363–7.
- [6] Mul D, Bertelloni S, Carel JC, et al. Effect of gonadotropin-releasing hormone agonist treatment in boys with central precocious puberty: Final height results. *Horm Res* 2002;58:1–7.
- [7] Carel JC, Lahlou N, Guazzarotti L, et al. Treatment of central precocious puberty with depot leuprorelin. *Eur J Endocrinol* 1995;132:699–704.
- [8] Tanaka T, Niimi H, Matsuo N, et al. Results of long-term follow-up after treatment of central precocious puberty with leuprorelin acetate: Evaluation of effectiveness of treatment and recovery of gonadal function. *J Clin Endocrinol Metab* 2005;90:1371–6.
- [9] Klein KO, Barnes KM, Jones JV, et al. Increased final height in precocious puberty after long-term treatment with LHRH agonists: The NIH experience. *J Clin Endocrinol Metab* 2001;86:4711–6.
- [10] Jay N, Mansfield MJ, Blizzard RM, et al. Ovulation and menstrual function of adolescent girls with central precocious puberty after therapy with gonadotropin-releasing hormone agonists. *J Clin Endocrinol Metab* 1992;75:890–4.
- [11] Tonini G, Lazzerini M. Side effects of GnRH analogue treatment in childhood. *J Pediatr Endocrinol Metab* 2000;13:795–803.
- [12] Massart F, Parrino R, Placidi G, et al. Prolactin secretion before, during, and after chronic gonadotropin-releasing hormone agonist treatments in children. *Fertil Steril* 2005;83:719–23.
- [13] Chantilis SJ, Barnett-Hamm C, Byrd WE, et al. The effect of gonadotropin-releasing hormone agonist on thyroid-stimulating hormone and prolactin secretion in adult premenopausal women. *Fertil Steril* 1995;64:698–702.
- [14] Cedars MI, Steingold KA, Lu JH, et al. Pituitary function before, during, and after chronic gonadotropin-releasing hormone agonist therapy. *Fertil Steril* 1992;58:1104–7.
- [15] Amino N, Hidaka Y, Takano T, et al. Possible induction of Graves' disease and painless thyroiditis by gonadotropin-releasing hormone analogues. *Thyroid* 2003;13:815–8.
- [16] Sonoda M, Nagata Y, Inoue Y, et al. A case of transient hyperthyroidism during pseudomenopausal therapy. *Acta Obstet Gynaecol Jpn* 1999;51:857–960.
- [17] Fukata S, Kubota S, Ito M, et al. A case of painless thyroiditis occurred after administration of nafarelin. *Hormone Rinsho* 1999;47:90–2.
- [18] Kasayama S, Miyake S, Samejima Y. Transient thyrotoxicosis and hypothyroidism following administration of the GnRH agonist leuprolide acetate. *Endocr J* 2000;47:783–5.
- [19] Eyal O, Rose SR. Autoimmune thyroiditis during leuprolide acetate treatment. *J Pediatr* 2004;144:394–6.
- [20] Tanaka T, Umesaki N, Ogita S. Altered sensitivity to anti-endometriosis medicines in an adenomyosis patient with thyroid dysfunction. *Gynecol Endocrinol* 2000;14:388–91.
- [21] Redmond GP. Thyroid dysfunction and women's reproductive health. *Thyroid* 2004;14:S5–15.
- [22] Mazer NA. Interaction of estrogen therapy and thyroid hormone replacement in postmenopausal women. *Thyroid* 2004;14:S27–34.
- [23] Iughetti L, Predieri B, Ferrari M, et al. Diagnosis of central precocious puberty: Endocrine assessment. *J Pediatr Endocrinol Metab* 2000;13:709–15.
- [24] Aghini-Lombardi F, Antonangeli L, Pinchera A, et al. Effect of iodized salt on thyroid volume of children living in an area previously characterized by moderate iodine deficiency. *J Clin Endocrinol Metab* 1997;82:1136–9.
- [25] Anasti JN, Flack MR, Froehlich J, et al. A potential novel mechanism for precocious puberty in juvenile hypothyroidism. *J Clin Endocrinol Metab* 1995;80:276–9.
- [26] Cheung T, Lo KW, Lam CW, et al. A crossover study of triptorelin and leuprorelin acetate. *Fertil Steril* 2000;74:299–305.
- [27] Martino E, Bartalena L, Bogazzi F, et al. The effects of amiodarone on the thyroid. *Endocr Rev* 2001;22:240–54.